

# 6 Formation of Earth's Atmosphere and Oceans

In the previous chapters, we provided essential chemistry and physics of planetary atmospheres needed for the rest of the book. Now, we turn to the evolution of Earth's atmosphere – a topic that will occupy most of the following six chapters. Earth is, of course, the best-studied planet, and it is also the one of greatest intrinsic interest because it harbors life, including us. One of the great goals of planetary science, which we will discuss in Ch. 15, is to determine whether truly Earth-like planets exist around other stars and if they're inhabited. To pursue that investigation, we need to be well informed about how Earth's atmosphere evolved and what kept our own planet habitable. Here, we start at the very beginning of atmospheric evolution on Earth: the origin of the atmosphere.

## 6.1 Planetary Formation

### 6.1.1 Formation of Stars and Protoplanetary Disks

In 1755, Immanuel Kant (1724–1804) qualitatively proposed that the Solar System formed from gravitational collapse of a cloud of diffuse matter, and in 1796, Pierre-Simon Laplace (1749–1827) provided a rough scientific outline for this theory. Today, it is generally accepted that both stars and planets form from the collapse of interstellar clouds of gas and dust. In the case of the Solar System, the central parts of the cloud collapsed to form the Sun, and the remainder of the material was spun out by rotation into a flattened disk, called the *solar nebula* (Boss and Ciesla, 2014). What was originally an amorphous cloud flattened into a disk because matter contracting within the plane of rotation was resisted by gas pressure and centrifugal force (experienced within the co-rotating frame of reference), whereas matter contracting from above either pole of the initial cloud did so more easily, opposed only by gas pressure. Similar gaseous

nebulae around other stars are called *protoplanetary disks*. Such disks evolve in a few million years into *debris disks*, which consist of solid debris without the gas.

The nebula theory is supported by the detection of circumstellar nebulae and debris disks around young stars. For example, the Atacama Large Millimeter/submillimeter Array (ALMA) has revealed a pattern of dark and bright concentric rings at  $\sim 1\text{--}3$  mm wavelengths in a protoplanetary disk surrounding the star HL Tauri with a spatial resolution of a few AU (ALMA-Partnership *et al.*, 2015) (Fig. 6.1(a)). This 1.3 solar mass star is  $\sim 450$  light years away and  $\leq 1\text{--}2$  m.y. old. The dark rings are perhaps regions where planet formation is taking place. Whether gaps have been cleared by planets or are places where smaller solid grains are coagulating is unresolved at the time of writing. One suggestion is that some dark rings correspond to condensation of ices such as water (D1 in Fig. 6.1(a)) and ammonia hydrates (D2) (Blake and Bergin, 2015).

Figure 6.1(b) shows a Hubble Space Telescope visible wavelength picture of a debris disk 63 light years away around the star  $\beta$ -Pictoris. The visible part of the disk extends to over 100 AU from the star – well beyond the  $\sim 30$  AU orbit of Neptune in our own Solar System. The disk is warped due to perturbation from a large planet. Figure 6.1(c) shows an image obtained from the Very Large Telescope (VLT) in Chile operated by the European Southern Observatory (Lagrange *et al.*, 2010) using *adaptive optics* (a technique described in Sec. 15.2.1). The small bright dot to the upper left of the (dark) star is the planet,  $\beta$ -Pictoris-b, which has about 9 Jupiter masses, an orbital radius of 8–15 AU, and an effective temperature of  $1500 \pm 300$  K (Bonnefoy *et al.*, 2011).  $\beta$ -Pictoris is a bright, bluish main sequence star of spectral type A5V, which is about 1.75 times the Sun's mass and  $\sim 8\text{--}20$  million years in age. Consequently, this system is not a perfect analog for our own Solar System's

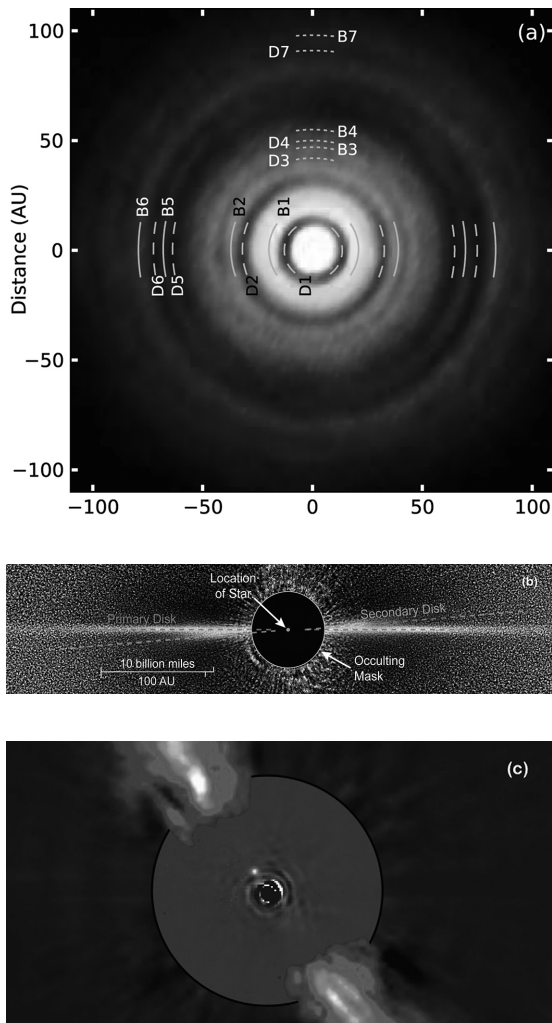


**Figure 6.1** (a) A pattern of bright concentric rings (labeled B1, B2, etc.) separated by dark rings (labeled D1, D2, etc.) around the star HL Tauri, imaged by the *Atacama Large Millimeter/submillimeter Array* (ALMA) at 1 mm wavelength. (Source: ALMA-Partnership (2015).) (b) The disk of Beta Pictoris seen in visible light by the *Hubble Space Telescope*. The central star is blocked out in the photo and a faint secondary disk, inclined at  $4^\circ$ , is seen in scattered light. (Courtesy of NASA, ESA.) (c) Near infrared photograph of Beta Pictoris taken by the *Very Large Telescope* (VLT) in Chile. The star is again blocked out. The white dot to the upper left of the star is an 8-Jupiter-mass planet aligned with the disk at 8 AU from the star. A separate disk image from ESO's 3.6 m telescope has been grafted onto the central VLT image in this photo. (Courtesy of ESO/ A.-M. Lagrange *et al.*) (A black and white version of this figure will appear in some formats. For the color version, please refer to the plate section.)

past; nevertheless, it provides direct evidence for planet formation in a circumstellar disk. Something similar happened around our own Sun, albeit on a somewhat smaller scale.

### 6.1.2 The Planetesimal Hypothesis

The exact steps in planet formation are still a matter of research. Most astronomers think that planet formation is initiated by *accretion* of solid materials that condenses from a disk. The term accretion refers to the process by which orbiting particles collide with each other, eventually forming *planetesimals*. Planetesimals are conventionally considered to be objects 0.1–10 km across but there are several competing models for planetesimal formation and some recent models form 100–1000 km planetesimals directly from centimeter-size pebbles or meter-scale boulders in the nebula in a single event. In the traditional model, a  $\sim 10$  km planetesimal has enough gravity to perturb the motion of other planetesimals and accrete mass from smaller ones. So bodies become fewer in number over time. In regions where growth of a few bodies outpaces the others, *runway accretion* leads a *planetary embryo* or *protoplanet* of diameter  $10^3$ – $10^4$  km, and eventually to planets.

The physics for the process of planetesimals accreting into planets originated with the astronomer Viktor Safronov (1917–1999) (Safronov, 1972). Rocky, *terrestrial planets* such as Venus and Earth are formed almost entirely from lumps of such solid material. *Gas giants* such as Jupiter and Saturn are thought to have solid cores that formed by accretion. Once these cores grew larger than about 10–15 Earth masses, though, they were able to capture more and more gaseous hydrogen and helium from the surrounding solar nebula in positive feedback (Inaba and Ikoma, 2003). The largest gas giant, Jupiter, grew to over 300 Earth masses and although it has a composition enriched in elements heavier than helium compared to the Sun (Guillot, 1999), most of the material, which is H or He, must have been captured gravitationally from the nebula. This process is the *core accretion model* of giant planet formation (e.g., Pollack *et al.*, 1996).

Some astronomers have argued that gas giant planets possibly formed by gravitational collapse of the disk itself (e.g., Boss, 2005, 2006, 2008, 2012; review by Helled *et al.*, 2014). In the cool outer regions of the disk, numerical simulations show that the gas can clump into Jupiter-sized objects within a few orbital periods. Whether this *disk instability* (DI) (or *gravitational instability*, GI) model is viable or not might be resolved if a spacecraft determines whether Jupiter really does have a core of rock and ice through detailed study of its gravitational field. But such analysis is challenging even for NASA's *Juno* orbiter mission because the core is only a few percent of the total mass (Helled *et al.*, 2011). Also, the result may not yield a definitive answer because cores can form even

in the GI model when grains entrained in the gas sediment out under gravity (Helled *et al.*, 2008).

Currently, not many astronomers favor the DI mechanism for forming planets partly because stars that have giant planets possess high metallicity, i.e., a relatively high abundance of elements heavier than H and He, which makes sense if rocky cores are important for giant planet formation (Fischer and Valenti, 2005; Johnson *et al.*, 2010). Planets of less than four Earth radii form over a wide range of host star metallicity (Buchhave *et al.*, 2012) but metallicity differences are still linked to the occurrence of rocky planets and gas dwarfs (Buchhave *et al.*, 2014; Wang and Fischer, 2015). Overall, evidence favors the *core accretion* model for forming both terrestrial and giant planets, but considerable uncertainty still exists and the core accretion and DI models may not be mutually exclusive or may each have roles under different circumstances.

The details of the planetary accretion process are not completely understood although various steps have been identified (e.g., reviews by Chambers (2014), Johansen *et al.* (2014), Lunine *et al.* (2011), Pfalzner *et al.* (2015), Raymond *et al.* (2014)). Initially, solid particles that condensed out of the solar nebula would have been gravitationally attracted to the nebular midplane, where they would have collided with each other and clumped together to form larger and larger particles. This is followed by four stages of growth: (1) planetesimal formation, (2) runaway growth, (3) oligarchic growth, and (4) late state accretion. Figure 6.2 shows the timescales

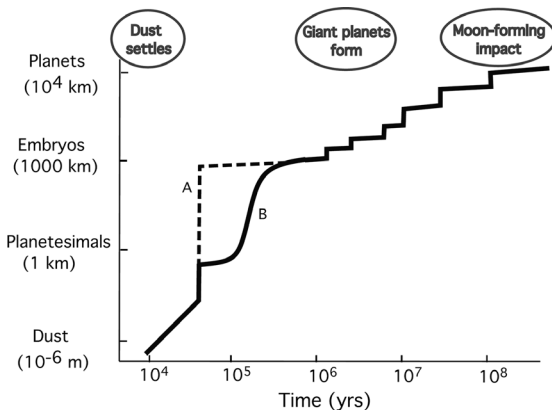


**Figure 6.2** A sketch showing the characteristic timescales and sizes of objects in the formation of objects in the Solar System. Path A is for a model where centimeter to meter-size objects clump quickly into planetary embryos. Path B represents the standard picture of *runaway growth* up to embryos. Paths A and B join around the *oligarchic growth* phase. (From Raymond *et al.* (2010). Reproduced with permission. Copyright 2010, John Wiley and Sons.)

associated with the size of objects at each stage. Stages (1)–(3) make planetary embryos in what we call the “traditional model.” A recent model, which we discuss below, suggests that the accretion of *pebbles* (centimeter-sized objects) can rapidly make embryos while gas is still in the disk, however (Jansson and Johansen, 2014; Lambrechts and Johansen, 2012).

The first phase of getting from centimeter-sized objects up to kilometer-sized planetesimals has generally been thought a theoretical challenge. Gas pressure slows the orbital motion of gas molecules more than large dust particles. So the fast-moving clumps experience a headwind, leading to orbital decay. Thus, gas drag can cause bodies to fall into the Sun. This process is fastest for meter-size objects, so the problem is called the *meter-size catastrophe* or *barrier* (Weidenschilling, 1977). Various mechanisms to overcome this difficulty have been suggested, including gravitational instability and clumping of bodies between turbulent eddies (Cuzzi *et al.*, 2008).

In fact, the physics of the so-called catastrophe may instead be a solution to planet formation. If a radial pressure bump arises in a nebula (e.g., from turbulence) pebbles should drift radially into the bump from both inner and outer sides (Jansson and Johansen, 2014; Whipple, 1972). If the pressure  $p$  varies with orbital radius  $r$  with gradient  $dp/dr$ , then on the inner side of a bump, where  $dp/dr > 1$ , gas has super-Keplerian velocity and particles are forced by the gas to move outward. In contrast, on the outer side where  $dp/dr < 1$ , the gas is sub-Keplerian and particles are dragged inward. Pebbles pile up at the bump and may induce core accretion (Chatterjee and Tan, 2014). Due to gas drag, capture of pebbles can rapidly form gas giant cores (Levison *et al.*, 2015).

In the traditional model, once planetesimals reached beyond a kilometer in size, the remaining three steps of the accretion process are reasonably well understood. Two key factors in the growth of larger bodies are called *gravitational focusing* and *dynamical friction*. The collision cross-section of a given body is enhanced beyond the geometric cross-section by a gravitational focusing factor,  $F_g$ ,

$$F_g = 1 + \frac{v_{\text{esc}}^2}{v_{\text{rel}}^2} \quad (6.1)$$

where  $v_{\text{esc}}$  is the body’s escape velocity (proportional to a body’s size for objects of the same density) and  $v_{\text{rel}}$  is the relative velocity of nearby accreting bodies. Most encounters do not lead to collisions, but gravitational tugs change the orbits of planetesimals. *Dynamical friction* is the statistical process by which large bodies involved in many encounters tend to acquire circular, co-planar orbits, while

small bodies are perturbed into eccentric, inclined orbits. Because the orbits of larger planetesimals remain nearly circular, they tend to pass each other slowly so that  $v_{rel}$  is small and  $F_g$  is large, enhancing the likelihood of collision. So, this growth stage is called *runaway growth*. During this phase the largest planetesimal in each orbital zone consumes most nearby planetesimals. These large planetesimals, though, still represent only a small fraction of the total mass. Runaway growth ends once the mass of the largest bodies becomes gravitationally important, probably when they reach the range of  $10^{-5}$ – $10^{-3}$  Earth masses.

When each region of the disk contains a single planetary embryo, along with numerous small planetesimals, the third growth stage, called *oligarchic growth*, begins. Runaway growth slows and larger embryos stir up the velocities of nearby planetesimals more than smaller ones, so that smaller embryos catch up in their growth. During oligarchic growth, the embryo “feeding zones” are about 10 Hill radii in width. The Hill radius defines a sphere within which a body’s gravity is more influential for the motion of another body than is the Sun’s gravity. Hence, a Hill radius is defined as a function of the ratio of the mass of the body,  $M$ , to the mass of the sun,  $M_{\odot}$ :

$$r_{Hill} = a \left( \frac{M}{3M_{\odot}} \right)^{1/3} \tag{6.2}$$

where  $a$  is the semi-major axis of the orbit around the Sun. As an aside, the Hill radius is equivalent to the distance of the  $L_1$  Lagrange point, which lies along a line between the Sun and a body in its orbit. At the  $L_1$  point for the Earth, for example, the gravitational pull of the Earth is just enough that a body at  $L_1$  feels less effective gravity from the Sun and orbits in 1 year with the same

angular velocity as the Earth. Inserting masses into eq. (6.2), the Hill radius of the present Earth is  $\sim 1\%$  of an AU; for Jupiter,  $r_{Hill} \sim 0.3$  AU.

Oligarchic growth ends when planetary embryos contain about half of the solid mass in a particular region, while the other half resides in planetesimals (Kenyon and Bromley, 2006). The result is the formation in  $\sim 10^5$  years of Moon-to-Mars-sized embryos at 1 AU and in  $\sim 10^6$  years of protoplanetary cores of 1–10 Earth masses beyond 4 AU. These cores then sweep up nebula gas and become giant planets within a few million years. When many planetesimals are lost, dynamical friction lessens, so embryos excite the eccentricities and inclinations of other embryos, as shown in Fig. 6.3. With less gravitational focusing, the rates of collisions become more infrequent. So, a prolonged,  $\sim 10^8$  year phase of *late-stage accretion* ensues for the terrestrial planets, which involves giant impacts with bodies the size of the Moon or Mars. We’ll return to this point below, as it has important consequences for the formation of Earth’s ocean and atmosphere. Thus, during late-stage accretion, embryos coalesce into inner planets through embryo–embryo collisions. The Earth, for example, probably formed from the collisional accretion of tens of Moon to Mars-sized bodies.

The traditional accretion theory described above presumes that the disk of dust and gas was largely gone during the latter stages of accretion in the terrestrial planet zone. This scenario is self-consistent, as the timescale for the dissipation of such disks, a few million years (Alexander *et al.*, 2006; Haisch *et al.*, 2001; Hartmann *et al.*, 2005; Russell *et al.*, 2006), is shorter than the time scale for the final assembly of rocky planets, which is  $\sim 30$ – $100$  million years (Fig. 6.2).

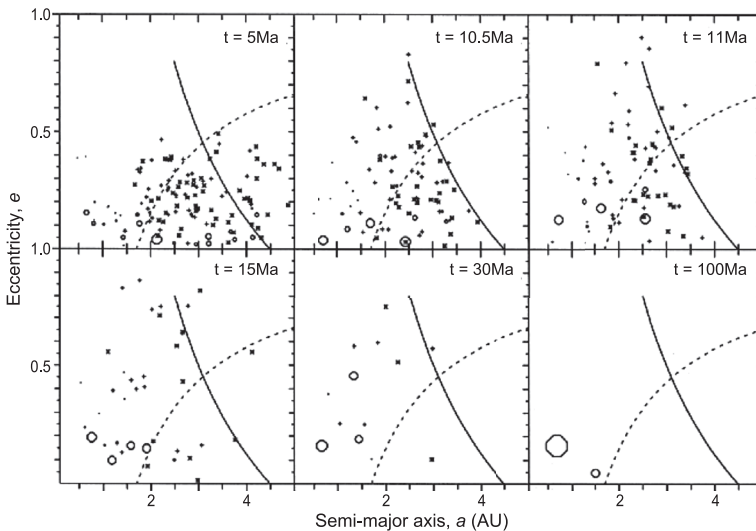


**Figure 6.3** Snapshots of the accretion process taken at various intervals, according to the model of Morbidelli *et al.* (2000). (Reproduced with permission. Copyright 2000, John Wiley and Sons.) This particular model was initialized with 5.5 Earth masses of planetary embryos distributed between 0.7 and 4 AU, along with 100 asteroids of negligible mass. Asteroids with initial semi-major axes  $a$ , of 2–2.5 AU are shown as crosses, whereas those with initial semi-major axes beyond 2.5 AU are denoted by asterisks. The solid and dashed curves represent the boundaries of the present-day asteroid belt, with aphelion ( $a(1+e)$ ) and perihelion ( $a(1-e)$ ) distances corresponding to 4.5 AU and 1.7 AU, respectively, where  $e$  is eccentricity.

Jupiter had to form much faster than the inner planets in order to capture large amounts of gas from the nebula. A factor that favored accretion is that Jupiter should have formed beyond the *ice line* (or *snow line*) in the nebula, where water ice could condense. Oxygen is the third most abundant element in the Sun,  $\sim 0.05\%$  by number, and so condensation of  $\text{H}_2\text{O}$  ice would have provided relatively large amounts of solid material, thereby allowing the accretion process to proceed quickly at Jupiter's orbital distance. Also, Jupiter's greater distance from the Sun allowed a wider feeding zone for a proto-Jupiter, following eq. (6.2). Water ice was also available farther out in the nebula, but the orbital times were longer, and so Saturn, Uranus, and Neptune accreted less solar nebula material. Indeed, the latter two planets are commonly termed *ice giants*, as opposed to *gas giants*, as they are both strongly depleted in H and He compared to the Sun.

### 6.1.3 Planetary Migration: When Did the Gas and Dust Disappear?

An alternative line of thought about accretion models, sometimes called the *Hayashi school*, was developed in Japan. Chushiro Hayashi and those who followed him assumed that the *terrestrial* planets grew to large sizes in the presence of significant dust and gas (Hayashi *et al.*, 1979; Hayashi *et al.*, 1985). In this model, accretion proceeds faster with dust and gas present. When applied to our own Solar System, the model implies that Earth's primordial atmosphere should have contained gas of solar composition. As we discuss below, data from noble gases suggest that the present atmosphere was not derived directly from a gas of solar composition. But it is possible that a single large impact event (e.g., the Moon-forming impact) that occurred late during the accretion process could have removed an earlier solar-composition atmosphere. So, the Hayashi model cannot be easily dismissed on these grounds.

Many models for Earth's final assembly have concentrated on the gas-free accretion scenario. The bulk of the atmosphere and oceans must then have formed from solid materials that condensed out of the solar nebula and were present in the planetesimals from which Earth formed. Observations of exoplanets, though, show that not all planetary systems form in the same way. About 0.5%–1% of Sun-like stars have *hot Jupiters* – giant planets orbiting very close ( $< 0.5$  AU, typically 0.04–0.05 AU) to their parent stars (Howard, 2013). It should be impossible to form giant planets at very small distances because of the high temperature of the gas, tidal disruption, and Keplerian shear where material closer to

star orbits faster than material farther away. Hence, such planets must have formed farther out and then *migrated* in to closer orbital distances (reviewed by Chambers (2009)). Such migration is possible only in the presence of substantial gas and dust in the disk. So, the accretion process proposed by the Hayashi school may well apply to other planetary systems. In our own Solar System, the contribution from gas-assisted accretion versus planetesimal accretion may vary in the different formation regimes of terrestrial planets, asteroids, or objects beyond the ice line (e.g., Johansen *et al.*, 2015).

Planet migration also occurs in some recent models of the Solar System. In the *Grand Tack* model, Jupiter migrates inward to 1.5 AU during the first 0.6 m.y., then back outward to  $\sim 5$  AU once Saturn forms (Hansen, 2009; O'Brien *et al.*, 2014; Walsh *et al.*, 2011). Such migration can stunt the growth of Mars by truncating the distribution of solids beyond 1 AU. Producing a small Mars has proved challenging for other planet formation models.

In general, we should keep an open mind about how our Solar System actually formed. We will hopefully learn much more about this process over the next few decades from observing what has happened around other stars.

## 6.2 Volatile Delivery to the Terrestrial Planets

In this book, we are primarily concerned with how planetary atmospheres form and evolve. A key issue, then, is how did the Earth obtain its *volatiles*? Volatile compounds, to an atmospheric scientist, are those that have relatively low melting or boiling points, so that they are present as liquids or gases in a planet's hydrosphere or atmosphere. Key volatiles for the Earth include  $\text{H}_2\text{O}$ , carbon, nitrogen, and sulfur. These (plus phosphorus) are also the so-called "SPONCH" elements from which life is made.

### 6.2.1 The Equilibrium Condensation Model

Astronomers and planetary scientists have been concerned with the question of volatile delivery ever since they started thinking about how planets might be built. One early thinker on this topic was John Lewis (of MIT and then University of Arizona). Lewis developed the *equilibrium condensation model* for planetary formation (e.g., Lewis and Prinn, 1984). In this model, Lewis assumed that a nebula of gas and dust that had the same overall composition as the Sun surrounded the growing protosun. Lewis also assumed that the solar nebula contained the same amount of mass as the Sun – an estimate

that may be too high by at least a factor of 10 – but we can ignore this aspect of his model, because it has only a weak effect on his predictions. (A nebula that includes more than about 0.1 solar masses would have rapid transport of most of the mass inwards onto the central star, together with radial expansion of the remaining disk and is unlikely to evolve to the present Solar System.) The basic idea is that initially the solar nebula is hot for a variety of reasons: high density prevents radiation from the protosun escaping, friction within the nebula generates heat, and gravitational potential energy has been converted to kinetic energy during infall of material. After reaching a peak temperature, the nebula cools. The order in which different materials should condense from such a nebula as it cools is shown in Table 6.1. In summary, the condensation sequence begins with highly refractory metals and oxides, and this is followed by Ni–Fe metal, silicates, sulfides, hydrated minerals, and finally, ices.

The *refractory* metals and oxides near the top of Table 6.1 are compounds that vaporize only at extremely high temperatures, >1500 K. The species making up the lower part of the list below silicates are volatile compounds with relatively low vaporization temperatures. Missing from the table are H<sub>2</sub> and He, which condense only at extremely low temperatures, and hence were probably always present in the solar nebula as gases.

Lewis proposed that the list of Table 6.1 explains much of what we observe about the composition of planets in our own Solar System. The terrestrial planets formed closer to the Sun, from silicates and iron–nickel alloy, which are the compounds that could condense in the warm inner parts of the solar nebula. In Lewis's model, the nebula became cool enough somewhat interior to 5 AU to allow H<sub>2</sub>O to condense out as water ice; hence this distance is called the *ice line* (or *snow line*), as mentioned previously (Fig. 6.4). The presence of Jupiter at 5.2 AU from the Sun is thus nicely explained in Lewis's model. In the current Solar System, water-rich (~10 wt%) asteroids occur beyond ~2.7 AU (Gradie and Tedesco, 1982).

The Lewis model also purports to explain why Earth has some water (~0.1 wt%) whereas Venus does not. According to Fig. 6.4, Earth forms just outside the region where hydrated silicates should have condensed out of the nebula (represented in Fig. 6.4 by tremolite (Ca<sub>2</sub>Mg<sub>5</sub>Si<sub>8</sub>O<sub>22</sub>(OH)<sub>2</sub>) and serpentine ((Mg, Fe)<sub>3</sub>Si<sub>2</sub>O<sub>5</sub>(OH)<sub>4</sub>)). Venus, by contrast, is well inside of this boundary. With a little tweaking of the nebula temperature profile, Earth would have received water from this mechanism, whereas Venus would not. So, for many years, Lewis and his colleagues argued for a dry origin for Venus.

**Table 6.1** Materials that condense from the nebula as it cools. The shading of rows indicates chemical groups of substances. Note that the exact equilibrium condensation temperature depends on assumptions about total pressure and nebula composition. Here a pressure of 10<sup>-4</sup> bar is assumed (Lodders, 2003).

Temp/ K	Substance	General groups (Comments)
~1800	Highly refractory metals, W, Os, Ir, Re	<i>Refractory metals</i>
1677	Corundum, Al <sub>2</sub> O <sub>3</sub>	<i>Refractory oxides</i>
1593	Perovskite, CaTiO <sub>3</sub>	
1397	Spinel, MgAl <sub>2</sub> O <sub>4</sub>	
1360	Nickel–iron metal, Ni, Fe	<i>Ni–Fe (core-forming metals)</i>
1347	Pyroxene, CaMgSi <sub>2</sub> O <sub>6</sub> (diopside)	<i>Silicates (rock-forming minerals)</i>
1354	Olivine, Mg <sub>2</sub> SiO <sub>4</sub> (forsterite), or Fe <sub>2</sub> SiO <sub>4</sub> (fayalite)	(60% of Earth's crust)
<1000	Alkali feldspars, (Na, K)AlSi <sub>3</sub> O <sub>8</sub>	
~700	Troilite, FeS	<i>Sulfides.</i> (Chalcophile (sulfur-loving) elements also include Zn and Pb).
550–330	Minerals with –OH or H <sub>2</sub> O in their formulae	<i>Hydrated minerals</i>
Ionic substances above ▲, Molecular substances below ▼		
~180	Water ice, H <sub>2</sub> O	<i>Ices</i> (Caveat: The form in which C or N condenses depends upon the availability of water and kinetics. If there is not enough water, they will not condense as clathrates, e.g., graphite could condense at higher temperature (Lodders, 2003).)
~120–130	Ammonia ice, NH <sub>3</sub> ·H <sub>2</sub> O	
40–78	Methane ice, CH <sub>4</sub> ·7H <sub>2</sub> O or CH <sub>4</sub> ice	
50–60	Nitrogen ice, N <sub>2</sub> ·6H <sub>2</sub> O and N <sub>2</sub> ·7H <sub>2</sub> O	

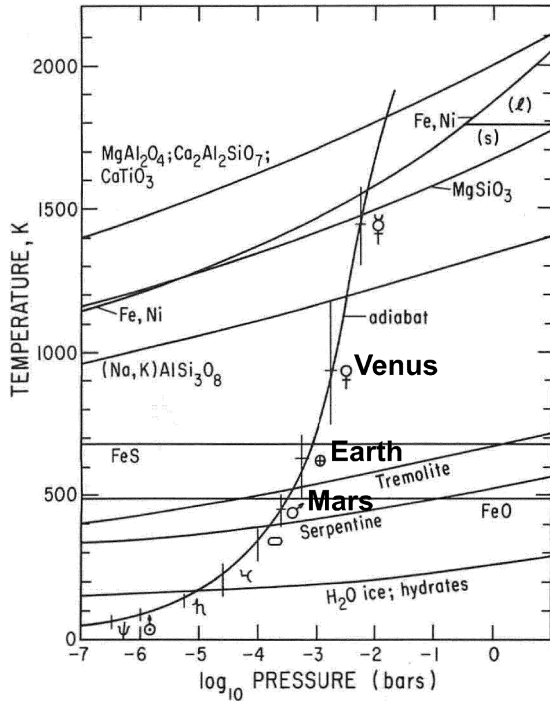


**Figure 6.4** Diagram illustrating the equilibrium condensation model of planetary formation. The curved line running through the middle represents an adiabat extending radially along the mid-plane of a  $1M_{\text{Sun}}$  solar nebula. The other curves represent boundaries at which various minerals would condense, assuming solar composition for the nebula. Standard astronomical symbols mark the planets. (From Lewis and Prinn (1984), p. 61.)

The equilibrium condensation model for planetary formation is no longer considered viable, for a number of reasons. For one, radial mixing of planetesimals during the latter stages of accretion means that Earth and the other terrestrial planets are composed of material that originally condensed over a wide range of orbital distances. This provides other mechanisms by which Earth may have obtained its water, as discussed further below. Of equal importance is the fact that hydrated silicates are now considered kinetically difficult to form (Prinn and Fegley, 1989). Chemical reactions between gaseous and solid materials proceed extremely slowly at these relatively low temperatures. Hydrated silicates are indeed found in meteorites, but they are now thought to have formed by alteration of silicate minerals by liquid water within meteorite parent bodies (Bunch and Chang, 1980). Thus, many of the detailed predictions of the equilibrium condensation model are no longer accepted. However, the simple prediction of why our Solar System contains rocky planets on the inside and gas or ice giants farther out is still an important success.

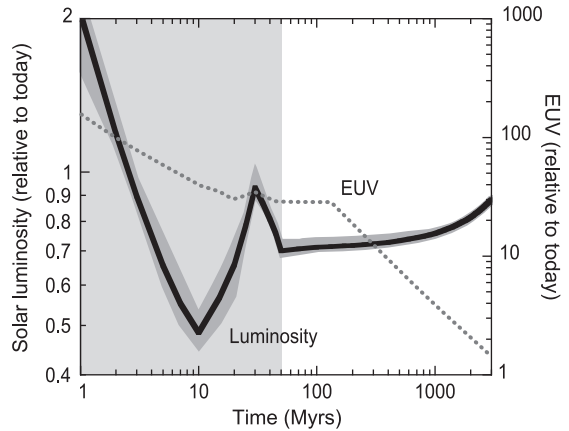


**Figure 6.5** Changes in luminosity for the Sun's first 3 billion years. A time of zero corresponds to the age of the Solar System of 4.5673 Ga. The shaded region is the pre-main sequence time. The shaded path shows the probable solar luminosity, with its spread giving the uncertainty. (Adapted from Zahnle *et al.* (2007). Reproduced with permission of Springer. Copyright 2007, Springer Science + Business Media B.V.)

One further nuance of the Lewis model concerns the early history of solar luminosity (Zahnle *et al.*, 2007). The Sun has steadily brightened since it settled down onto the *main sequence* (Sec. 2.1.2) at  $\sim 4.52$  Ga (see Ch.11 for climatic implications of this brightening). By convention, the Solar System formation clock starts ticking at the age of the oldest objects, which are calcium-aluminum inclusions (CAIs) in chondritic meteorites, dated at  $4.5673 \pm 0.0002$  Ga (Amelin *et al.*, 2010; Connelly *et al.*, 2016). During the  $\sim 50$  m.y. of pre-main-sequence time from then until 4.52 Ga, solar luminosity changed considerably as the Sun contracted and then went through nuclear fusion ignition (Fig. 6.5). This period of time happens to correspond to planet formation, and so would have affected volatiles. For example, at 1 AU, water was in the form of vapor at 2 m.y. but was in the ice phase at 10 m.y. when solar luminosity went through a minimum. These issues remain to be fully explored in planet formation models. Where the snow line was during the nebula phase also depends upon how rapidly the nebula cooled, which depends upon assumed opacities (Lesniak and Desch, 2011; Mulders *et al.*, 2015).

### 6.2.2 Modern Accretion Models

With the development of faster computers, the simulations of accretion have become more detailed. One illustrative simulation is shown in Fig. 6.6. This particular calculation extended from the Sun to 5 AU. That was enough to include the four innermost planets in our own

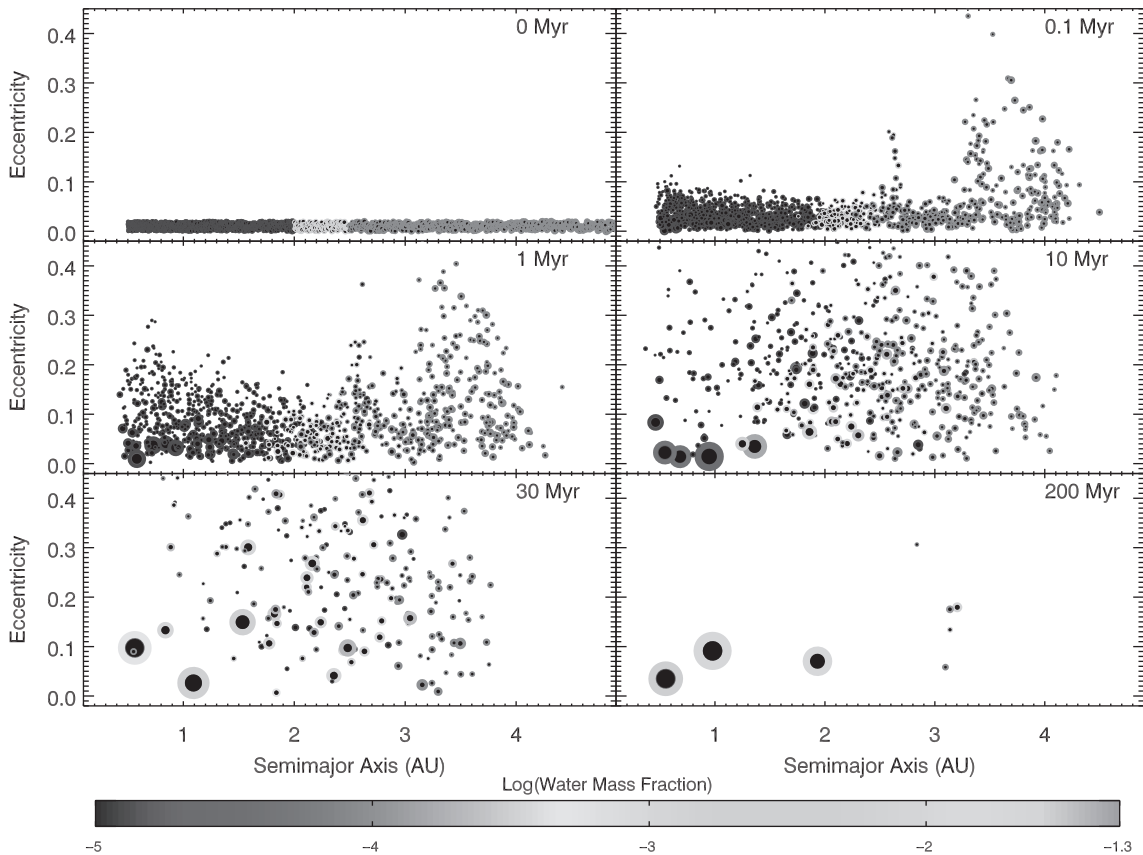


**Figure 6.6** Snapshots of a particular rocky planet accretion simulation for the region inside 5 AU around the Sun. The horizontal axis is the planet's semi-major axis, i.e., its mean distance from the Sun. The dots represent large planetesimals, some of which will grow into planetary embryos and planets. The position of the dot on the vertical axis indicates the planetesimal's eccentricity. The size of the dot indicates the mass of the planetesimal or planet, and its color shows the fraction of its total mass that is made up of water. The simulation was terminated after 200 million years. (From Raymond *et al.* (2006).) (A black and white version of this figure will appear in some formats. For the color version, please refer to the plate section.)

Solar System, but not the four giant planets. The calculation started from a swarm of 1886 planetesimals of various sizes, the average mass being about half the mass of the Moon. These planetesimals were initially assumed to be orbiting at various distances from the Sun, randomly picked between 0.4 and 5 AU (top left panel). The initial eccentricities and inclinations of the orbits were assumed to be zero. (Orbital eccentricity is defined in Sec. 2.2.1. The inclination is the angle of the planet's orbital plane with respect to the average, or *invariant*, plane of the system.) A Jupiter-mass planet, not shown, was assumed to be on a circular orbit just outside the calculation, at 5.5 AU. The colors of the dots represent the water content of the planetesimals, with blue showing water-rich bodies and red representing dry ones. The planetesimals change from red to blue going from a few tenths of an AU out to

5 AU. Water-rich planetesimals containing 5% water by mass are present beyond 2.5 AU.

Several interesting phenomena occur in such simulations, only a few of which will be mentioned here. Within a few hundred thousand years following the start of the simulation shown, the planetary embryos began to drift both inwards and outwards from their initial positions, and they were excited to higher eccentricities and inclinations. All of this happened because of the way they perturb each other gravitationally. Most importantly, water-rich planetesimals from beyond 2.5 AU were scattered inward towards the inner parts of the planetary system. Some of these ended up being incorporated into planets that remain close to the Sun. In this particular simulation, a 2-Earth-mass planet formed at 0.98 AU, very close to Earth's actual orbital distance. Besides

being considerably larger than the real Earth, this planet was also much more water-rich. The fraction of Earth's total mass that is water (including water in Earth's mantle) is estimated around 0.1 wt% (see Sec. 6.3), which would make it yellowish-green in this figure. By contrast, the blue planet in the figure has a water mass fraction close to  $10^{-2}$ . Such a planet, if it existed, would have oceans that were 30–40 km deep, as compared to only about 3–4 km on Earth.

The simulation shown in Fig. 6.4 also produced a 1.5-Earth-mass planet at 0.55 AU and a 1-Earth-mass planet at 1.9 AU. Both of these planets also have lots of water. The innermost one, though, is well inside the inner edge of the liquid water *habitable zone*, as we will see later on in Ch. 15. If such a planet formed in a real planetary system, it would probably lose its water by the runaway greenhouse mechanism described in Ch. 13. The outermost planet is close to, or beyond, the outer edge of the habitable zone, and so any water on that planet's surface may be frozen, depending upon the strength of the greenhouse effect of its atmosphere and the planet's albedo.

The key point from this simulation and others like it is that the planets formed within the inner parts of planetary systems can be either much wetter or much drier than Earth. That is because some planets just happen to incorporate large, water-rich planetesimals from outside 2.5 AU, whereas other planets do not. Once again, the results are

stochastic. If one does many simulations, though, and counts the terrestrial planets that are formed, one finds more that are water-rich than water-poor (Raymond *et al.*, 2004). Hence, if these simulations realistically represent planetary formation, there should be lots of rocky planets with at least as much water as Earth.

### 6.2.3 D/H Ratios and Their Implications for Water Sources

Another potential source of water and other volatiles is comets. Comets are small bodies with diameters ranging from kilometers to tens of kilometers that are composed of roughly equal mixtures of ice and rock. They originate from beyond Neptune's orbit (~30 AU). The comets that we observe today come from two regions: the *Oort Cloud* or the *Kuiper Belt* (see Fig. 6.7). The Oort Cloud is a spherical shell of  $10^{12}$ – $10^{13}$  comets surrounding the Solar System that extends outward to roughly 100 000 AU, or approximately 1.6 light years, beyond which the Sun's gravitational influence can be overcome by other stars (Levison and Dones, 2014). The Oort Cloud is the source of most *long-period comets*, many of which are observed only once. The orbits of these comets are randomly distributed in space and are nearly parabolic, indicating that their source region must be spherical and extremely distant. The *Kuiper Belt* is a donut-shaped reservoir of comets that lies within the plane of the Solar System,

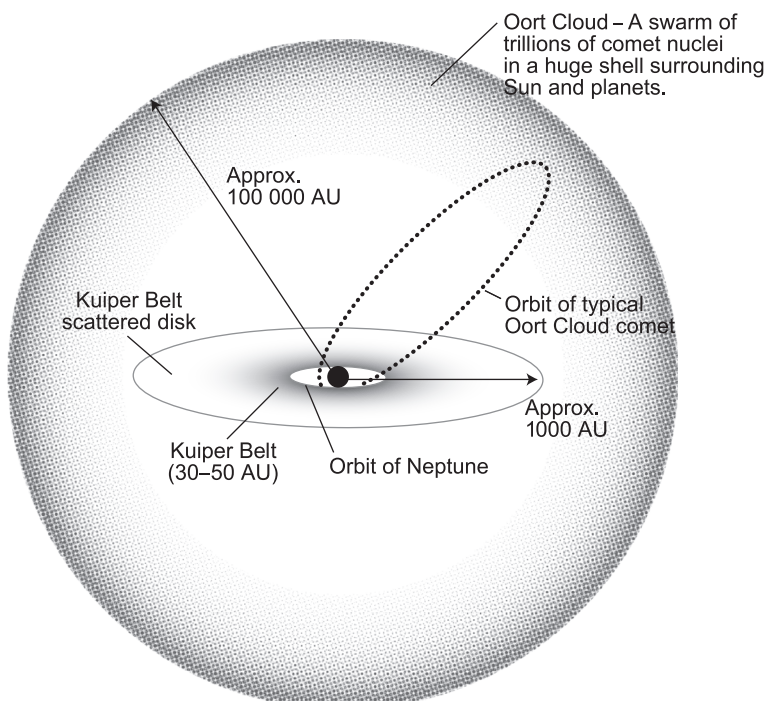


**Figure 6.7** Diagram illustrating the relationship of the Oort Cloud and the Kuiper Belt to the Solar System. The orbit of a typical Oort Cloud comet is shown.

but beyond the orbit of Neptune, between 30–50 AU with scattered objects out to ~1000 AU. It is estimated to contain over 70 000 objects with size exceeding 100 km and is the source of most *short-period comets*, many of which are in low-inclination orbits that are prograde (i.e., in the same direction that the Sun rotates and that the planets orbit).

Because they contain large amounts of water ice, comets could, in principle, have been the source of Earth's water. This idea was popular amongst planetary scientists for many years (see, e.g., Chyba, 1987), especially as it might also explain the abundance pattern of noble gases in Earth's atmosphere (Owen *et al.*, 1992). We'll return to this issue in Sec. 6.4. Comets also contain other volatile materials, including complex organic carbon compounds, and so some scientists (Chyba, 1990; Oro, 1961) have suggested that they might have contributed directly to the origin of life. The main problem with this latter idea is that the proportion of interesting organic molecules that survive impact with the Earth is very small (Pasek and Lauretta, 2008; Pierazzo and Chyba, 1999).

Over the past two decades, the idea that comets supplied most of Earth's water has fallen out of favor. One reason is that the deuterium to hydrogen ratio became known for different Oort Cloud comets: Halley,

Hyakutake, Hale-Bopp, 2002T7, and Tuttle. The D/H ratio of terrestrial seawater has a value of  $(1.558 \pm 0.001) \times 10^{-4}$ . The D/H ratio in the five aforementioned Oort Cloud comets average about twice that value (Hartogh *et al.*, 2011b; Robert, 2001). Consequently, Oort Cloud comets could not have accounted for most of the Earth's water. As we will discuss in more detail in Ch. 13, the D/H ratio in a planet's atmosphere can increase with time if the planet loses hydrogen faster than it loses deuterium, but it cannot go back in the other direction. However, comet 103P/Hartley 2 has a D/H ratio of  $(1.6 \pm 0.24) \times 10^{-4}$ , similar to Earth's oceans (Hartogh *et al.*, 2011b). This object is a *Jupiter-family comet* (JFC), which means that it is a short-period comet in the ecliptic plane sourced from the Kuiper Belt. However, its nitrogen isotope ratio does not support the idea that JFCs contributed significantly to Earth's water. The Earth has a  $^{15}\text{N}/^{14}\text{N}$  ratio of  $3.678 \times 10^{-3}$  whereas the ratio measured in HCN and CN in 103P/Hartley 2 (and all other comets) is ~1.8 times higher. By contrast, chondritic meteorites (see below, Sec. 6.3), which come from the asteroid belt, have an average D/H ratio that is close to that of Earth's oceans. For example, carbonaceous chondrites have  $\text{D/H} = (1.4 \pm 0.1) \times 10^{-4}$  (Fig. 6.8) (Marty and Yokochi, 2006), and their  $^{15}\text{N}/^{14}\text{N}$  ratio is also comparable to the

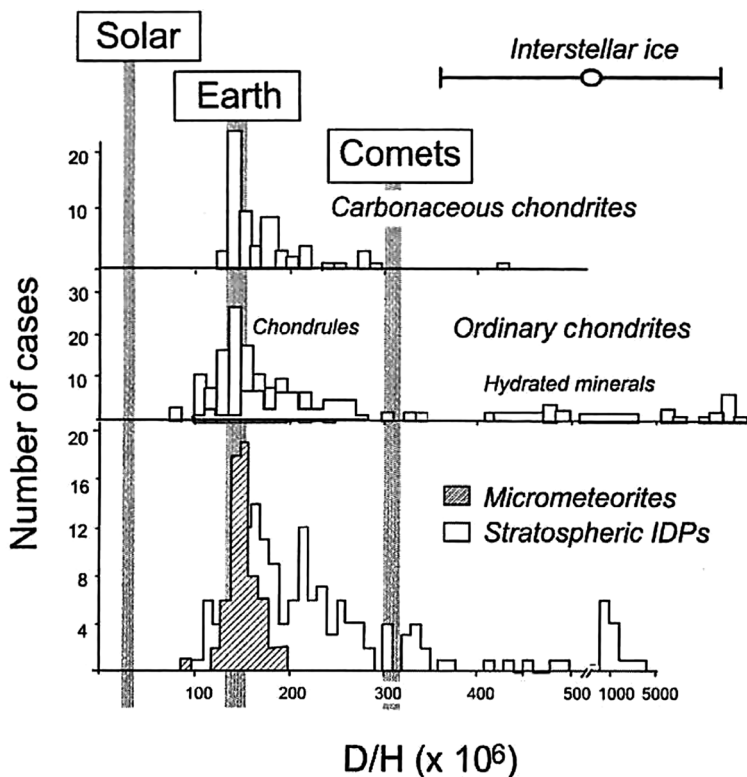


**Figure 6.8** The deuterium/hydrogen (D/H) ratio in different reservoirs of the solar system. The vertical gray lines show the Sun, Earth, and Oort Cloud comets. From top to bottom, the histograms show values for carbonaceous chondrites, ordinary chondrites, and micrometeorites and Interplanetary Dust Particles (IDPs). (From Marty and Yokochi (2006). Reproduced with permission. Copyright 2006, The Mineralogical Society of America.)

bulk Earth's. Furthermore, measurements on 67P/Churyumov–Gerasimenko (a JFC) by the *Rosetta* spacecraft show a  $D/H = (5.3 \pm 0.7) \times 10^{-4}$ , which is  $\sim 3$  times higher than on Earth (Altwegg *et al.*, 2015). So, overall the data are consistent with the idea that planetesimals from the asteroid belt region were the major source of Earth's water. In fact, isotopic and mass balance suggests that comets could have contributed no more than  $\sim 10\%$  of the Earth's water (Dauphas *et al.*, 2000).

A second strike against comets as the main source of Earth's water is that whereas abundant asteroids are expected to be scattered into the inner solar system, only about 1 in 3 million comets hits the Earth after Jupiter forms (Levison *et al.*, 2001). Thus, an unfeasible number of comets would need to have been scattered for the Earth to have accreted its ocean solely from such bodies (Zahnle, 1998).

Finally, we note that asteroids and comets lie on a continuum from warm, rocky planetesimals with no ice in the inner solar system to cold, ice-rich planetesimals far from the Sun. The asteroid–comet division is therefore one of taxonomic convenience rather than absolute distinction.

### 6.3 Meteorites: Clues to the Early Solar System

In considering the formation of the Solar System, we assumed that the nebula had the same composition as

the Sun. Direct evidence supports this idea. The composition of the Sun is known, at least partially, through spectroscopy, while *chondritic* meteorites (defined below) have preserved the composition of the nebula because they are leftovers of planet formation. The chondrite and solar compositions match, excluding gas-forming elements lost from the meteorites and lithium consumed on the Sun during nuclear reactions (Fig. 6.9).

Traditionally, meteorites were divided into three categories: (1) *irons*, which are predominantly iron and thought to be pieces of metallic asteroid cores, (2) *stony*, which are mostly silicates, and (3) *stony-irons* which are a mixture of silicates and iron that presumably sampled both asteroid mantles and cores. However, more recently, meteorites have been classified into *chondrites*, *achondrites* and *primitive achondrites*, as shown in Fig. 6.10, because this classification better reflects their origins (Weisberg *et al.*, 2006).

Meteorite classification depends on composition. Chondrites are often defined as containing *chondrules*, which are globules of silicate minerals, up to a few millimeters in size, interpreted as rounded particles of rapidly cooled silicate melt formed by condensation or re-melting of dust in the solar nebula. However, some chondrites do not contain chondrules. So, a more general definition of a chondrite is a meteorite with nearly solar-like composition, excluding the gas-forming elements. Achondrites do not contain chondrules and are pieces of

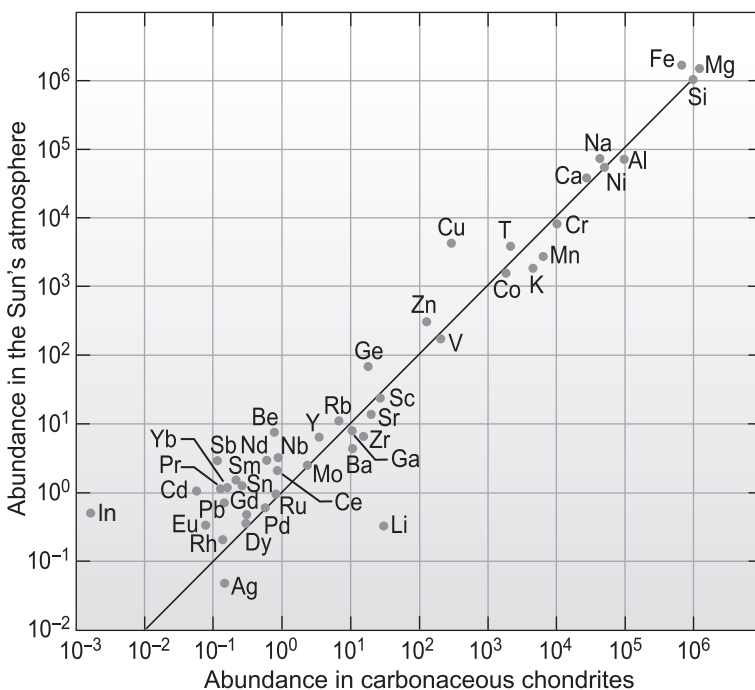


**Figure 6.9** The close match between the elemental abundance determined from spectroscopic measurements of the solar photosphere and the CI carbonaceous meteorites. Data are normalized such that Si =  $10^6$ . Lithium (Li) is more abundant in CI carbonaceous chondrites than the Sun because this element is used in solar nuclear fusion. (Adapted from McBride and Gilmour (2004), p. 37.)

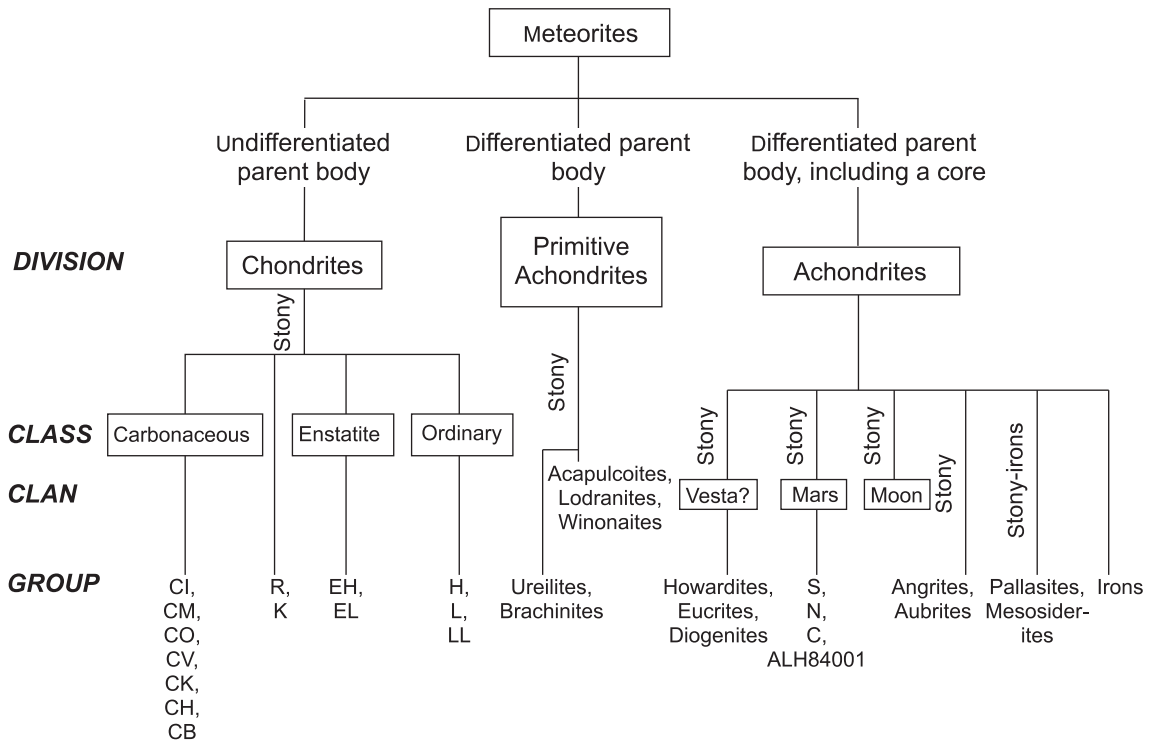


Figure 6.10 The classification of meteorites (simplified).

igneous rock that crystallized from magmas or lavas of parent bodies that had differentiated into a core, mantle, and crust. They include meteorites from Mars, the Moon, the asteroid Vesta, and other unknown differentiated asteroids. The third division shown on Fig. 6.10, the *primitive achondrites*, contains meteorites from asteroids that were heated to the point of melting but not of large-scale differentiation when a metallic core formed.

Below the three divisions of Fig. 6.10, the nomenclature can get complicated and include classes, clans, groups, and subgroups. For simplicity, we show only some key terminology. Three important classes of chondrites are as follows.

- *Ordinary chondrites*, which contain 5–15 wt% Fe–Ni, and make up 97% of all chondrites in the worldwide meteorite collection. Some geochemists think of these chondrites as similar to the bulk composition of the Earth, albeit imperfectly because the Earth has no perfect match to any chondrite or achondrite (Drake and Righter, 2002).
- *Carbonaceous chondrites*, contain organic compounds with CI and CM groups at 2–3.5 wt% C, and others with less, CK ~0.1 wt% C and CH ~0.8 wt% C. The CH and CB groups are also relatively rich in metals at 40–50 wt% Fe compared to 18.2 wt% Fe in CI.

- *Enstatite chondrites*, so named because they contain enstatite ( $\text{MgSiO}_3$ , a pyroxene mineral) as the dominant silicate mineral. They also contain an average of  $20 \pm 9$  wt% metal and are notable for being the only chondrite class that has a wide variety of elements with isotope compositions identical to the Earth (Javoy *et al.*, 2010). Amongst these, carbonaceous chondrites appear least processed, which means that while parent body processes, such as aqueous alteration, may have destroyed minerals, the elemental composition has remained intact. They haven't experienced element segregation because the ratios of their non-volatiles elements (such as Fe, Si, Mg, Al, Ca) match those in the Sun. The CI chondrites have this similarity for all but the most volatile elements, so that CI chondrites are regarded as the most chemically primitive.

One aspect of meteorite composition, which is important in discussing the origin of the Moon (Sec. 6.8) and explaining how we know that certain meteorites are from Mars (Ch. 12), concerns the relative proportions of stable oxygen isotopes,  $^{16}\text{O}$ ,  $^{17}\text{O}$ , and  $^{18}\text{O}$ . These differ in the bulk composition of celestial bodies according to where the bodies formed. One idea to account for this trend is that photodissociation of nebula gases (particularly CO) fractionated the isotopes of oxygen in a way that

depended upon distance from the Sun (Clayton, 2002; Lyons and Young, 2005; Thiemens, 2006; Thiemens and Heidenreich, 1983). Subsequent condensation into solids caused the variation of the oxygen isotopes with heliocentric distance to be preserved.

However, exactly how the O isotopes fractionated may be more complicated. At least some of the models have CO photodissociation taking place far from the inner Solar System, with the liberated oxygen later transported inwards in the form of water ice or some other O-bearing species. In these models, the isotopic differences between Earth, Mars, and the various meteorite types must have arisen at a later stage sometime during planet formation. There also does not seem to be a clear trend with heliocentric distance: ordinary and carbonaceous chondrites lie in opposite directions in O isotope space compared with Earth. Nonetheless, the oxygen isotopes in meteorites serve as a geochemical fingerprint for their provenance. For example, if the O isotope ratios in the bulk silicate of a meteorite match those from the clan of meteorites known to come from Mars (because they contain inclusions of Martian air), they serve as acceptable proof that the meteorite is also Martian.

The volatile content of meteorites is important because such volatiles ended up composing the Earth's atmosphere, ocean and life (e.g., Fegley and Schaefer, 2010). Water in the oceans and crust is ~0.03% of the Earth's mass. Estimates for how much water is inside the Earth vary but a few oceans worth in the mantle is typical, e.g., Lecuyer *et al.* (1998) estimate 0.3–3 oceans, equivalent to an extra 0.008–0.08 wt%. More recent estimates for Earth's bulk water are higher, 0.1%–0.3 wt% (Marty, 2012). We can compare ordinary chondrites, which contain ~0.1 wt% C, ~0.03 wt% N, and ~0.3 wt% water. The CI meteorites in Fig 6.10 are the most volatile-rich of the carbonaceous chondrites and contain an average of 3.5 wt% C, 0.3 wt% N, and up to ~10 wt% water (Fegley and Schaefer, 2010; Kerridge, 1985). It is possible that many planetesimals that went on to form Earth had already melted and differentiated (e.g., Kruijer *et al.*, 2014), and were not primitive objects like chondrites, and so had lost most of their volatiles. But the volatile abundance of the Earth can be explained if only a small proportion of our planet was accreted from volatile-rich chondritic material contained in either planetesimals or embryos scattered into the inner solar system. Indeed, planet formation models predict such scattering and show that embryos can contribute most of the water (Fig. 6.6). Volatiles inside embryos and planetesimals are expected to vaporize into gases during accretion in the process of *impact degassing*, as we describe below in Sec. 6.5.

## 6.4 The Implications of the Abundances of Noble Gases and Other Elements

Aside from the accretion of solids, the gravity of planetary embryos larger than Mars would have been enough to capture some nebula gas, mostly H<sub>2</sub> and He (Inaba and Ikoma, 2003). But today, the atmospheres of Venus, Earth, and Mars do not resemble solar composition at all, and they could not have been directly derived from a solar gas, as we discuss in more detail below. For now, and to illustrate the problem, suppose that the atmosphere of a terrestrial planet had started out with a solar composition and that hydrogen and helium escaped to space. In this case, primordial methane and ammonia would have been oxidized to CO<sub>2</sub> and N<sub>2</sub> with the loss of hydrogen, and the result would be an atmosphere of roughly 60% CO<sub>2</sub>, 20% Ne, and 10% N<sub>2</sub>, with a remainder of minor gases. This composition is not observed in any terrestrial planet atmosphere, with neon being strikingly underabundant (e.g., 18 ppmv in the Earth's atmosphere). Consequently, the present atmospheres on the rocky planets are described as *secondary atmospheres*. This distinguishes them from *primary atmospheres* of solar composition captured from the nebula, such as the atmosphere of Jupiter, or atmospheres directly descended from solar composition in the way that we just described.

### 6.4.1 Atmospheres, Geochemical Volatiles, and Refractory Elements

In thinking about the origin of atmospheres, it is useful to divide up the chemical elements into volatile and refractory elements. *Refractory* elements are those that tend to stay in solid compounds with very high melting and boiling points, e.g., Fe. We can sub-categorize the volatile elements into *geochemical volatiles*, such as K, Zn, or Cl, which are volatile at moderately high temperatures, and *atmosphiles*, which are elements that tend to form liquids or atmospheric gases at typical planetary temperatures. Examples of liquids are Earth's oceans and liquid methane in Titan's polar lakes. The most important atmosphiles are C, H, O (at least in H<sub>2</sub>O or CO<sub>2</sub>), N, and the noble gases.

If we examine the average composition of Venus, Earth, and Mars, we can compare the abundance of some elements to the solar abundance (Fig. 6.11). We then see that all three inner planets are depleted in geochemical volatiles compared to the Sun, although Mars is less depleted, presumably because Mars formed farther out in a cooler part of the solar nebula where geochemical volatiles, such as chlorine, were more abundant (Wänke

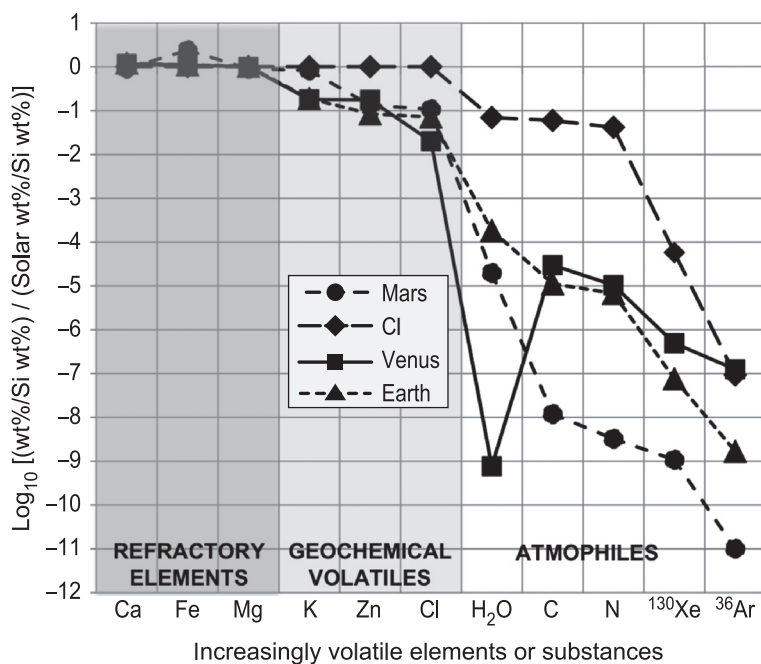


**Figure 6.11** The relative abundance of some refractory, geochemical volatile, and atmophile elements and substances in the average compositions of CI carbonaceous chondrites, Venus, Earth, and Mars compared to solar abundance. Following convention, both solar and planetary compositions are normalized to the Si mass fraction. Data sources: solar abundance from Anders and Grevasse (1989), noble gas data from Pepin (1991), CI meteorite C and N abundance from Fegley and Schaefer (2010), elemental model compositions of Mars and Venus from Lodders and Fegley (1998), and elemental model composition of Earth from McDonough (2003).

and Dreibus, 1994). While we see that all atmophiles are depleted many orders of magnitude compared to solar abundances, the relative abundance of atmophiles differs greatly for Venus, Earth, and Mars.

Atmophile contrasts between Venus, Earth, and Mars provide clues to the divergent fates of their atmospheres. For example, the lack of water on Venus (only ~40 ppm in its atmosphere) is explained by its loss through a runaway greenhouse effect, which we describe in Ch. 13. In Ch. 12, we also discuss how the general lack of atmophiles on Mars can be explained mostly by their escape to space. This, of course, is a consequence of Mars' small mass (~1/9 of an Earth mass) and low gravity. For all the terrestrial planets, the depletion of atmophile elements relative to solar abundance suggests that direct capture of atmospheres of solar composition from the solar nebula cannot explain the composition of present atmospheres on the terrestrial planets. Patterns of noble gas abundance provide additional evidence for how terrestrial planet atmospheres formed (e.g., Moreira (2013), Halliday (2013)), as we now discuss.

#### 6.4.2 Noble Gases

The noble gases, He, Ne, Ar, Kr, and Xe are unreactive and so are the strongest atmophiles. Their condensation temperatures are so low that they should have remained as atomic gases throughout the solar nebula, at least within the orbit of Neptune. On planets, primordial noble gases

ought to reside in atmospheres rather than solids, except to the degree that they have been trapped in planetary interiors either because they were dissolved from primary atmospheres in melted rock during planetary accretion or were part of primary accretion material that was implanted by the solar wind.

The Nobel prize-winning chemist Francis Aston first described the evidence for loss of a primary atmosphere when he quantified the extreme scarcity of the noble gases compared to the other elements on the Earth (Aston, 1924). Modern data, similar to those of Aston, are shown in Fig. 6.12. We consider only nonradiogenic noble gases, i.e., gases that are *not* formed from the decay of parent radioactive elements. In Fig. 6.12, the amount of neon relative to nitrogen is especially notable. Nitrogen and neon should have been roughly similar in abundance in the solar nebula, but on Earth the Ne/N ratio is a tiny  $\sim 10^{-5}$ . Clearly, the noble gases contribute a minuscule amount to the mass of the Earth compared to other elements. Consequently, the Earth either did not take up the gaseous component of the solar nebula or it lost it, otherwise Ne/N would be about unity. So, the Earth must have accreted its present atmophiles from solids. Studies of meteorites suggest that C and N were largely brought in by organic material (e.g., Bergin *et al.* (2015)), while water was delivered as ice or in hydrous minerals (Sec. 6.3, above).

In a similar manner, we can examine the abundances of noble gas isotopes on Venus and Mars from data obtained by the *Viking* landers for Mars and the *Pioneer*

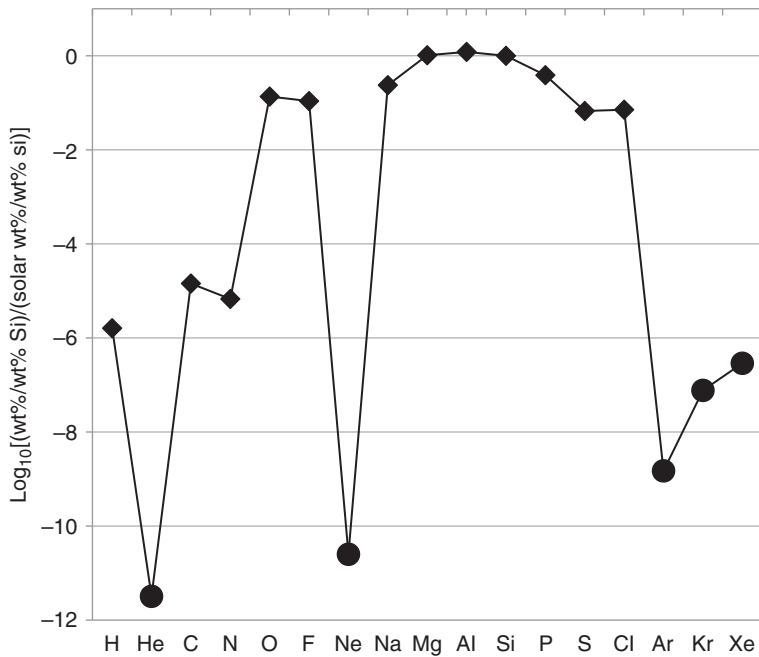


**Figure 6.12** Relative abundances of various elements on Earth compared to the Sun. Abundances are normalized to the abundance of Si on the Earth and Sun, respectively. Data show the ratio of Earth/Sun normalized abundances. Noble gases (filled circles) are very depleted compared to other elements (filled diamonds). Data: solar abundance from Anders and Grevasse (1989), noble gases from Pepin (1991), and elemental composition for Earth from Lodders and Fegley (1998).

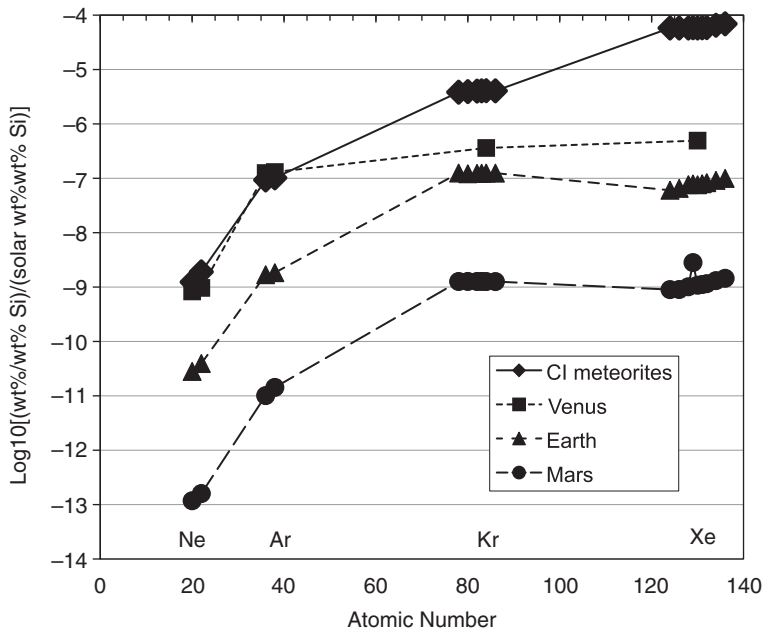


**Figure 6.13** Abundances of noble gas isotopes in CI carbonaceous chondrites and terrestrial planets relative to their solar abundance. Abundances are normalized to Si, as indicated on the vertical axis. Xenon isotopes on Earth and Mars are clearly mass-fractionated. Mars also has an unusually high relative abundance of the  $^{129}\text{Xe}$ , formed from the radioactive decay of  $^{129}\text{I}$ . Data from Pepin (1991) and references therein.

*Venus* and *Venera* spacecraft for Venus (Fig. 6.13). We exclude helium because this element escapes to space easily from rocky planets. In Fig. 6.13, the huge depletion of noble gases on Mars and Venus compared to solar abundance implies that these planets accreted volatiles as solid compounds, just like the Earth did. Another common aspect between the three terrestrial planets in

Fig. 6.13 is that the noble gases are generally increasingly enriched with greater atomic mass, which suggests that lighter gases have escaped or that heavier gases were brought in more easily. In fact, stable isotope ratios in the terrestrial atmospheres, which generally are expressed as the heavy/light isotopes for a particular element, tend to be larger than their solar equivalents. This pattern can

often be explained by preferential escape of the lighter isotope to space, as we discussed in Ch. 5.

While the abundance patterns of noble gases for Venus, Earth, and Mars all have large depletions and broadly similar trends compared to solar abundances, distinctions between them provide clues to the origin of each atmosphere. For example, argon and neon abundances are unusual for Venus. Nonradiogenic argon ( $^{36}\text{Ar}$  and  $^{38}\text{Ar}$ ) on Venus exceeds the chondritic abundance (Fig. 6.13), whereas neon approaches it. To put it another way, argon and neon are 70 and 20 times more abundant on Venus than on Earth, respectively. Why? One possibility is that Venus, by chance, accreted a big (>600 km) Kuiper Belt comet, where cold temperatures of <30 K and <17 K allowed argon and perhaps neon to condense as an ices, respectively (Owen and Bar-Nun, 1995). The probability of such a cometary accretion is fair, about 1 in 4 (Zahnle, 1998). A second explanation relies on the idea that during late accretion, early Venus experienced a *runaway greenhouse effect* (defined in Sec. 13.4) during which all its water was vaporized into a thick atmosphere. Under such circumstances, numerical simulations show that giant impacts would fail to remove components of a Venusian primary atmosphere, whereas on the Earth, explosive conversion of a liquid ocean to steam by giant impacts would transmit the shock to the atmosphere, causing atmospheric escape to take away noble gases previously captured from the nebula (Genda and Abe, 2005).

Radiogenic argon,  $^{40}\text{Ar}$ , provides clues to Venus' atmospheric and interior evolution. Argon-40 is produced from the radioactive decay of  $^{40}\text{K}$  with a half-life of 1.25 b.y., and so should gradually accumulate in an atmosphere if outgassing is efficient. Indeed, this is the reason why argon is the third most abundant gas in the Earth's atmosphere. However, Venus' atmosphere has only ~1/4 of the  $^{40}\text{Ar}$  found in the Earth's atmosphere. A possible explanation is that Venus is not efficiently outgassed, so its volcanism must have been relatively quiescent for most of its history, whereas Earth's volcanism was more or less continuous as a consequence of plate tectonics. It turns out that tectonics and volcanism underpin the long-term climate stability and volatile recycling needed for a biosphere (Ch. 11), so if life ever existed on an early, clement Venus, we can surmise that it would have been geologically short-lived.

The isotopes of xenon and neon on Earth and Mars are also fractionated, as shown by the slope of the closely packed data points in Fig. 6.13. These slopes are possibly informative about atmospheric evolution. They suggest an episode of early atmospheric escape driven by the extreme ultraviolet (EUV) radiation from the early Sun,

which was hundreds of times greater than today (e.g., Claire *et al.*, 2012), as shown in Fig. 6.5. We discussed these issues further in Sec. 5.11.2. For now, we will just consider how noble gas and geologic data imply that much of the atmosphere and hydrosphere on the Earth was formed relatively quickly.

### 6.4.3 Early Degassing

We have discussed how volatiles were accreted as part of solids, so that the Earth's atmosphere and ocean must have been made from volatiles released from the Earth's interior, but there has been historical debate about how quickly this happened. The process by which gases are released from solids to form the atmosphere and the ocean is called *degassing* or *outgassing*. An old view promoted by the geologist William Rubey was that volatiles degassed onto an almost airless body that had lost its primary atmosphere so that the ocean and secondary atmosphere built up gradually (Rubey, 1951, 1955). This idea is now seen as incorrect because volatiles would have been rapidly degassed to the surface of the Earth during accretion, as we describe below in Sec. 6.5. Indeed, various lines of evidence support early degassing. That said, Rubey was right about other things, as we shall discuss in Ch. 7.

Unequivocal geological evidence shows that oceans were present in the early Archean. The data come from the Isua area in West Greenland, which preserves a ~3.8 Ga belt of layered sedimentary and volcanic rocks (e.g., Nutman, 2006). Although the rocks have been heated up to several hundred degrees Celsius and compressed to pressures of thousands of bar by metamorphism, they provide evidence for material originally deposited under water. First, they include *pillow basalts* (Komiya *et al.*, 1999), which were formed when submarine volcanic lava erupted and squeezed out underwater like toothpaste to form bulbous, pillow-like structures. Second, some sediments were laid down on the seafloor or in shallow water according to their sedimentology and geochemistry (Moorbath *et al.*, 1973; Nutman *et al.*, 1997). There is also evidence of marine life because graphite grains in the sedimentary rocks are enriched in  $^{12}\text{C}$ , which is consistent with their derivation from microbes that tend to concentrate  $^{12}\text{C}$  (Ohtomo *et al.*, 2014; Rosing, 1999). Overall, the Isua rocks confirm that the Earth had acquired oceans, an atmosphere, and probably life when it was only 700 million years old.

More subtle geochemical evidence suggests that oceans were present even earlier at ~4.3 Ga. Fragments of 4.5–4.0 Ga crust persist as small (<0.5 mm) *zircons*, which are grains of zirconium silicate ( $\text{ZrSiO}_4$ ) (reviewed

by Harrison, 2009). Zirconium silicate is so durable that it remains even after its parent rock has vanished through erosion. Particularly old zircons, >4.0 Ga, are found embedded in a fossilized gravel bar called the Jack Hills conglomerate in western Australia. These zircons contain inclusions of quartz, which imply their production from silica-rich igneous rocks such as granites before 4.0 Ga. Thus, the zircons are possible evidence for continental rocks. But they also provide evidence for oceans. The zircons are enriched in  $^{18}\text{O}$ . Typically, surface rocks acquire an enrichment of  $^{18}\text{O}$  when surface waters weather them to produce clay minerals. It is well known from more modern rocks that this  $^{18}\text{O}$ -enrichment can be passed on to igneous rocks if the clay-rich surface rocks are buried and melted. So, these ancient zircons imply that liquid water existed on the surface of the Hadean Earth and that continental rocks not only existed but were being recycled through weathering and transport (Cavosie *et al.*, 2005; Mojzsis *et al.*, 2001; Trail *et al.*, 2007; Wilde *et al.*, 2001).

Noble gases also suggest early degassing (Allegre *et al.*, 1987). The present fluxes of primordial noble gases are far too slow to account for their amount in the atmosphere today (Holland, 1984; Tajika, 1998). For example, the current outgassing flux of  $^{36}\text{Ar}$  is a factor of ~4400 too slow to account for the amount of  $^{36}\text{Ar}$  in Earth's atmosphere if it had been added at that rate over geologic time. Consequently, most of the  $^{36}\text{Ar}$  was put into the atmosphere during an earlier time at a high outgassing rate. Indeed, the reason for such a small flux of  $^{36}\text{Ar}$  today is that the primordial noble gas isotopes (such as  $^3\text{He}$ ,  $^{20}\text{Ne}$ ,  $^{36}\text{Ar}$ , and  $^{130}\text{Xe}$ ) are severely depleted in mantle-derived rocks compared to atmospheric values, consistent with the idea of early degassing. By contrast, the isotopes such as  $^{40}\text{Ar}$  that are derived from radioactive decay are enriched inside the solid Earth. For example, the Earth's atmospheric value of  $^{40}\text{Ar}/^{36}\text{Ar}$  is 298.6, which is roughly a hundred times smaller than the upper mantle ratio of  $^{40}\text{Ar}/^{36}\text{Ar}$  of  $32\,000 \pm 4000$  and 27 times smaller than values from mantle plumes, such as ~8000 for Hawaii (Trieloff *et al.*, 2003). This suggests that  $^{36}\text{Ar}$  was outgassed early, while  $^{40}\text{Ar}$  accumulated over time in the mantle from decay of  $^{40}\text{K}$ , which has a 1.25 b.y. half-life. In fact, the  $^{40}\text{Ar}/^{36}\text{Ar}$  ratio of  $143 \pm 24$  in 3.5 Ga quartz inclusions suggests that considerable K was extracted from the mantle into crust in the Archean (Pujol *et al.*, 2013), consistent with other indications of early crust (e.g., Iizuka *et al.*, 2015). However, not all the  $^{40}\text{Ar}$  produced from decay has outgassed and about half remains in the Earth's interior (Marty, 2012; Turner, 1989), depending upon an assumed inventory of  $^{40}\text{K}$ .

In the atmosphere, some noble gases that are daughter products of comparatively short-lived radionuclides are notably missing, which suggests that they were released early and escaped to space. The best example is  $^{129}\text{Xe}$ , which has the radioactive parent  $^{129}\text{I}$  with a half-life of 15.7 m.y. Let us use a standard notation and denote the xenon-129 derived from radioactive decay of  $^{129}\text{I}$  as  $^{129}\text{Xe}^*$  to distinguish it from solar xenon. During the first 110 m.y. of Earth history, which corresponds to seven half-lives of  $^{129}\text{I}$ , 99% of the  $^{129}\text{Xe}^*$  would have been produced. The amount of  $^{129}\text{Xe}^*$  trapped in the minerals of chondritic meteorites tells us that the ratio of original  $^{129}\text{I}$  relative to the stable  $^{127}\text{I}$  isotope was  $\sim 10^{-4}$ . An estimate for the amount of  $^{127}\text{I}$  in the *bulk silicate Earth*<sup>1</sup> is 11 ppb by mass (Kargel and Lewis, 1993), so that after full decay of all  $^{129}\text{I}$  in the Earth, we should expect  $3 \times 10^{13}$  moles of  $^{129}\text{Xe}^*$  to have been produced. But the Earth's atmosphere contains only  $4.2 \times 10^{12}$  moles of  $^{129}\text{Xe}$  and only ~7% of this, or  $2.9 \times 10^{11}$  moles, is estimated to be from the decay of  $^{129}\text{I}$ , while the rest is solar and non-radiogenic (Pepin, 2000). Hence ~99% of radiogenic  $^{129}\text{Xe}^*$  – the amount produced during the first 110 m.y. – is missing. Thus,  $^{129}\text{Xe}^*$  appears to have outgassed early and to have been lost during or shortly after 110 m.y. It is unlikely that  $^{129}\text{Xe}^*$  was gradually lost later in Earth history because xenon is the heaviest (non-anthropogenic) gas in the atmosphere and is currently unable to escape. However, the process of hydrodynamic escape (see Sec. 5.10), which is thought to have been driven by the much higher extreme ultraviolet (EUV) output from the young Sun, might account for such xenon loss.

One other scenario that is sometimes invoked by geochemists to explain an apparent decoupling between atmospheric noble gases and those in the mantle is called a *late veneer*. The idea is that atmospheric noble gases were probably lost during the Moon-forming impact, and that they may have been replenished by material that was accreted later, particularly cometary material that arrived during the late heavy bombardment (see Sec. 6.7). Stable krypton and xenon isotopes ( $^{82,84,86}\text{Kr}$  and  $^{124,126,130}\text{Xe}$ ) measured in well gases that are thought to represent upper mantle composition lie on a mixing line between isotopically heavy carbonaceous chondrite material and air, and are distinct from solar values (Holland *et al.*, 2009). This suggests that the mantle derived its noble gases from an accreted component similar to

<sup>1</sup> The term *bulk silicate Earth* means “mantle + crust + hydrosphere” and is synonymous with “primitive mantle,” which is the theoretical reservoir that differentiated into a crust, depleted mantle, and hydrosphere.

carbonaceous chondrites, whereas the atmosphere comes from a different source in which noble gases were depleted in the light isotopes. According to its proponents, a *late veneer* of cometary material could account both for isotopic components of the noble gases and a nearly solar Kr/Xe ratio in the atmosphere, as observed (Dauphas, 2003; Owen *et al.*, 1992).

## 6.5 Impact Degassing, Co-accretion of Atmospheres, and Ingassing

### 6.5.1 Laboratory Evidence for Impact Degassing

An effective mechanism for producing early degassing was the high-energy impacts that occurred during accretion. Planet formation models suggest that at least some of the bodies accreted by the Earth would have been rich in volatiles (Sec. 6.2.2). How much of this material would have been released during impact?

In the 1980s, Tom Ahrens and colleagues, as well as some Russian scientists, performed experiments in which they fired high-speed projectiles into mineral targets (Gerasimov and Mukhin, 1984; Lange and Ahrens, 1982, 1986). They discovered that the heat of impact shocks liberated volatiles, including water, from carbonaceous chondrites (Tyburczy *et al.*, 1986). Complete devolatilization was achieved at shock pressures of 20–40 GPa. Shock pressures can be related to the velocity of planetesimal impacts during accretion by assuming reasonable material properties for the planetesimals. According to theory, degassing becomes important for impact velocities exceeding  $5 \text{ km s}^{-1}$ , which occur for (Mars-sized) planetesimals,  $\sim 1/10$  of an Earth mass. On that basis, once the radius of the Earth reached about a third of its present value, a dense, steam atmosphere should have formed (Matsui and Abe, 1986a). Later studies showed that other gases would have also been released with a composition that depends mainly on the iron content of the accreting planetesimals (Hashimoto *et al.*, 2007; Schaefer and Fegley, 2010; Zahnle *et al.*, 2010), as we discuss below.

### 6.5.2 Formation of Steam and Reducing Atmospheres During Accretion

The steam atmosphere formed from impact degassing would have provided insulation for the heat flux deposited by impacts on the growing planet, along with a substantial greenhouse effect. Calculations by Matsui and Abe (1986b) showed that such a “thermal blanket” would have caused the entire surface of the planet to melt during the late accretion, creating a *magma ocean*. Actually, irrespective of the atmospheric thermal blanket, a magma

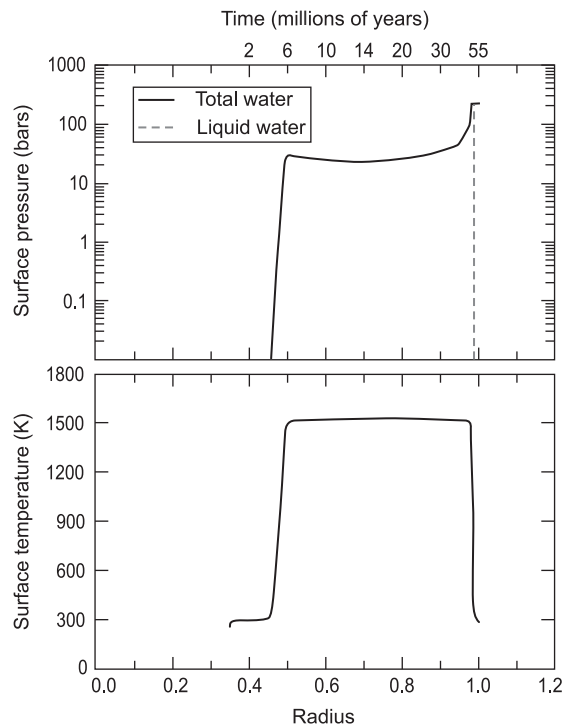


**Figure 6.14** The surface pressure and temperature for a model of impact degassing during accretion of the Earth. In this model, degassing exceeds escape to space when the growing planet reaches roughly 0.5 of an Earth radius. At that point, the atmosphere is opaque to the thermal infrared in a “runaway greenhouse” state and the surface melts. The steam atmosphere eventually collapses when the planet nearly reaches the current Earth radius. (Adapted from Zahnle *et al.* (1988) Reproduced with permission from Elsevier. Copyright 1988.)

consequence of giant impacts during late accretion (Tonks and Melosh, 1993). The surface pressure of the atmosphere at this time was controlled by the solubility of  $\text{H}_2\text{O}$  in the melt and should have been  $\sim 100$  bar.

Figure 6.14 shows the steam atmosphere model of Zahnle *et al.* (1988), which was similar to that of Matsui and Abe, except with more elaborate  $\text{H}_2\text{O}$  absorption coefficients. Related calculations including more detailed mineralogy and gaseous  $\text{CO}_2$  have also been published (Elkins-Tanton, 2008; Kuramoto and Matsui, 1996). Zahnle *et al.* explicitly kept track of the amount of water trapped inside the growing planet, along with exchange of water between the atmosphere and surface and escape of hydrogen to space. Because the hydrogen comes from water initially, such escape of hydrogen oxidizes the mantle. According to this calculation (Fig. 6.14, top panel), the atmospheric pressure increased from  $\sim 30$  bar to 240 bar right near the end of accretion, as the magma ocean solidified. This water then condensed out to form

$1.4 \times 10^{21}$  kg, is equivalent to a surface pressure of 270 bar; hence, this model ends up with  $\sim 90\%$  of the observed amount of surface water. About 140 bar of water was directly emplaced in the atmosphere by impacts; so subsequent outgassing provides roughly 100 bar of water, or about 40% of the modern ocean.

During impact degassing, other gases besides  $\text{H}_2\text{O}$  should have been released (Schaefer and Fegley, 2010; Zahnle *et al.*, 2010). If the infalling material had the composition of CI carbonaceous chondrites, equilibrium calculations at high pressure and temperature suggest that the gas composition would have been relatively oxidized, with  $\text{H}_2\text{O}$  and  $\text{CO}_2$  as the predominant constituents and minor  $\text{H}_2$  (Fig. 6.15 (b)). On the other hand, if accreting planetesimals were similar to ordinary chondrites,  $\text{H}_2$ -rich atmospheres with  $\text{CO}$  and  $\text{H}_2\text{O}$  as secondary components are expected, because of the presence of iron as a strong reducing agent (Fig. 6.15 (a)). So, the atmosphere during accretion could have been much more reduced than modern volcanic gases, whose relatively oxidized composition we discuss in Ch. 7.

### 6.5.3 Ingassing

Evidence suggests that the Earth has also experienced an opposite process from degassing, which is *ingassing*

(or *regassing*). Ingassing likely happened during accretion and has certainly occurred over geologic time from the subduction of volatile elements captured in sedimentary minerals.

If the proto-Earth grew larger than Mars in the presence of the nebula, it should have captured a *primary atmosphere* of nebular gas (Inaba and Ikoma, 2003), which would have partially dissolved in the molten surface produced by impacts (Fig. 6.16(a)). Subsequently, noble gases could have been trapped inside the Earth once molten material cooled. Evidence for solar noble gas might reside in  $^3\text{He}$  and neon (Harper and Jacobsen, 1996; Jacobsen *et al.*, 2008), which we consider in turn.

Helium has radioactive and primordial components. The two forms are: (1)  $^4\text{He}$ , which is present inside the Earth mainly as a consequence of radioactive decay in the mantle and crust of  $^{235}\text{U}$ ,  $^{238}\text{U}$ , and  $^{232}\text{Th}$ , and (2)  $^3\text{He}$ , which is a primordial remnant and thus relevant for this discussion. Helium diffuses easily, and  $^3\text{He}$  comes out of the mantle at a rate of  $3.7 \text{ kg yr}^{-1}$  (Schubert *et al.*, 2001, pp. 574–577). The inferred abundance of  $^3\text{He}$  in the deep Earth is similar to that in meteorites, so sometimes geochemists refer to the  $^3\text{He}$  as part of an *undegassed mantle reservoir* (Graham, 2002; Porcelli and Elliott, 2008). What this actually means is that  $^3\text{He}$  must have been

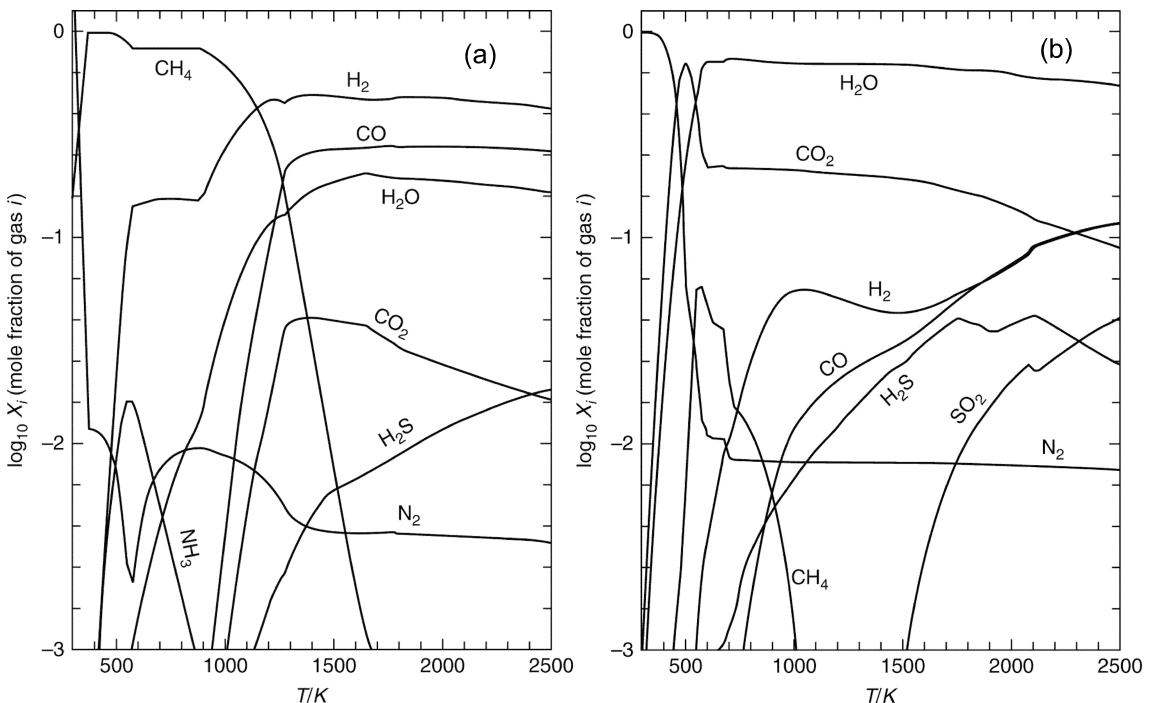


**Figure 6.15** (a) Strongly reducing atmospheres of accretion, calculated assuming gas compositions in equilibrium with CI chondrite composition at 100 bars. (b) Weakly reducing atmospheres of accretion, calculated assuming gas compositions in equilibrium with ordinary H-type chondrites at 100 bar. (From Zahnle *et al.* (2010) reproduced with permission from Cold Spring Harbor Laboratory Press.

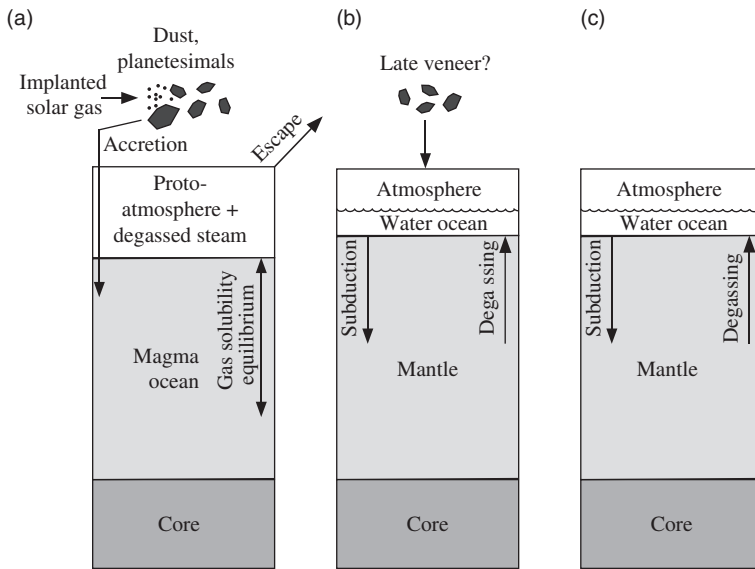


**Figure 6.16** Conceptual models of early to late atmospheres, following Jacobsen *et al.* (2008). (a) When the proto-Earth planetary embryo was larger than Mars, it could have captured a primitive atmosphere of solar composition. A magma ocean produced by impacts of accretion should have allowed a small fraction of the primitive atmosphere to dissolve in equilibrium, in the process of *ingassing*. Dust and planetesimals would have added a chondritic component to the growing Earth, including a possible solar component from implantation by the young solar wind. The hydrogen-rich primitive atmosphere was either eroded by the Moon-forming impact or escaped given the high flux of extreme UV from the young Sun. (b) The magma ocean froze into the mantle, possibly trapping a dissolved solar noble gas component of  $^3\text{He}$  and Ne. Collapse of the steam atmosphere from the Moon-forming impact and outgassing produced an ocean and atmosphere during the Hadean. Small imbalances between outgassing and subduction of sediments were likely important for returning carbon, nitrogen and sulfur atmospheres to the mantle. Possibly a “late veneer” of volatiles was added during Late Heavy Bombardment. (c) Subsequently, the atmosphere was maintained over geologic time by a balance between outgassing and ingassing.

added by a mechanism such as equilibrium dissolution of a primary atmosphere in a magma ocean because impact degassing ought to ensure that  $^3\text{He}$  could not have been accreted directly in solids (unless impact degassing is less than 100% efficient).

Evidence that neon may have dissolved in a magma ocean from a primary atmosphere in a similar way to helium comes from the inferred ratio of  $^{22}\text{Ne}/^{20}\text{Ne} \sim 12.5$  in the mantle, which is similar to  $^{22}\text{Ne}/^{20}\text{Ne} = 12.5 \pm 0.2$  in gas-rich meteorites (Porcelli and Wasserburg, 1995). However, any primary atmosphere was probably doomed. Vigorous escape to space of a hydrogen-rich primitive atmosphere is expected to remove it, and a *secondary atmosphere* formed from impact degassing would eventually dominate (Fig. 6.16(b)).

Once the Earth had a crust and liquid ocean (and after the Moon-forming impact, discussed in the next section), the ocean and atmosphere were maintained by a balance between ingassing of geologically transported volatiles

and outgassing from volcanoes and metamorphism (Fig. 6.16(c)). But some volatiles must have suffered an imbalance, perhaps during the Hadean eon represented by Fig. 6.16(b). Carbon, nitrogen, and sulfur have apparently partly returned to the mantle after early degassing. The ratio of carbon to  $^{36}\text{Ar}$  fluxes coming out of the mantle today is  $C/^{36}\text{Ar} \sim 8 \times 10^9$ , whereas the ratio of the total amount of carbon to  $^{36}\text{Ar}$  in the crust, atmosphere and ocean is only  $1.6 \times 10^6$ . At current rates, the surface reservoir of carbon would accumulate in 5 b.y., whereas the  $^{36}\text{Ar}$  would take an unfeasible 22 000 b.y. Clearly, the  $^{36}\text{Ar}$  degassed early, while it seems likely that carbon returned to the mantle after similar early degassing (Walker, 1990). The fate of most of the  $\text{CO}_2$  degassed into the atmosphere after the Moon-forming impact was probably to be incorporated into oceanic crust and subducted within  $\sim 10^8$  yrs (Zahnle *et al.*, 2007; Zahnle and Sleep, 2002). Others have suggested that organic carbon has been subducted into the mantle over geologic time (Hayes and Waldbauer, 2006).

Evidence suggests that significant amounts of nitrogen and sulfur have also been incorporated into sediments and subducted into the mantle. Measurements of mantle N correlate with  $^{40}\text{Ar}$ , the daughter product of radioactive  $^{40}\text{K}$ , which indicates that mantle N comes from subducted rocks in which  $\text{NH}_4$  substituted for  $\text{K}^+$  in minerals such as clays or micas (Goldblatt *et al.*, 2009; Marty and Dauphas, 2003). We discuss nitrogen further in Ch. 11. Tallying up the nitrogen inventories of the modern Earth suggests that almost ~60% of the nitrogen is in the mantle (Table 11.1). Sulfur isotopes and mass balance provide evidence that sulfur returned to the mantle as subducted sulfides. This process may have been efficient during the middle Proterozoic when rivers supplied the ocean with sulfate produced by oxidative weathering of continental sulfides, but the low-oxygen seafloor was conducive to the bacterial formation of sulfide, which could then be subducted (Canfield, 2004), as suggested earlier by Catling *et al.* (2002).

## 6.6 Moon Formation and its Implications for Earth's Volatile History

### 6.6.1 The Giant Impact Hypothesis

In the 1970s, various lines of evidence led to two independent suggestions that the Moon formed from the debris of a collision of a Mars-sized body (called *Theia*) with the proto-Earth (Hartmann and Davis, 1975; Jöns, 1985). One important finding from lunar samples brought back by the Apollo astronauts was that the Moon has a bulk composition similar to that of the Earth's upper mantle when we look at the major elements such as Si and Mg (Wänke, 2001). Also, the stable isotopes of oxygen  $^{16}\text{O}$ ,  $^{17}\text{O}$ , and  $^{18}\text{O}$  occur in the same relative proportions in the Earth and the Moon to a very high precision of several parts in a million (Herwartz *et al.*, 2014). The oxygen isotope ratios in bulk silicates of various celestial bodies vary depending on where the bodies were formed in the Solar System (Sec. 6.3 above). Thus, the oxygen isotopes suggest that the Moon and Earth have a common origin and that the Moon is not a captured object. Alternatively, turbulent mixing in the molten disk aftermath of the giant impact equilibrated the oxygen isotopes (Pahlevan and Stevenson, 2007). Tungsten and silicon isotope ratios are also nearly identical (Dauphas *et al.*, 2014).

By the late 1980s, the theory that the Moon formed as a result of a large collision with a Mars-sized object had gained acceptance (Stevenson, 1987). The theory, in brief, is that about 50–100 m.y. after the formation of the Solar System, *Theia* coalesced with the proto-Earth (both of which had already differentiated), causing much

or all of the Earth to melt (Kleine and Rudge, 2011). The likely age of this impact is ~4.47 Ga (Bottke *et al.*, 2015). Under such conditions, the density of molten iron caused it to separate into the Earth's core. However, the impact ejected considerable debris into orbit around the Earth from *Theia* material and the Earth's mantle. This debris accreted to form the Moon.

The giant impact theory explains several geochemical observations. The Moon's crust is depleted in *siderophile* elements by a factor of 0.2–0.003 compared with the Earth's crust and mantle. Siderophile elements, such as nickel (Ni), iridium (Ir), molybdenum (Mo), and germanium (Ge), are those that tend to be scavenged by metallic iron during melting. The impact model accounts for these data because there should be a low abundance of siderophile elements in the silicate mantle debris that gave rise to the Moon. Also, the Moon is poor in geochemical volatiles such as K and Rb by a factor of ~0.5 times terrestrial abundances (Taylor, 2001, p. 384). If the Moon formed from vaporized debris, then geochemical volatiles could have escaped.

The giant impact theory also explains geophysical observations. The Earth is comparatively high in its mean density in the trend of decreasing densities of the planets as a function of distance from the Sun, while the Moon is much less dense than the Earth (3.344 g cm<sup>-3</sup> vs. 5.515 g cm<sup>-3</sup>). These phenomena make sense if the Earth acquired iron from *Theia*'s core when the two bodies coalesced, leaving the Moon with a small, inner iron core only 240 km in radius beneath a ~90 km thick fluid shell (Weber *et al.*, 2011). This lunar core has an estimated <6 wt% light alloying components such as sulfur, as compared to up to ~10 wt% in the Earth's core (Birch, 1964; Poirier, 1994), again indicating the Moon's depletion of geochemical volatiles. The angular momentum of the Earth–Moon system is anomalously high compared to other planet–moon systems such that if all the lunar mass and momentum were put into the Earth it would rotate every 4 hours. Calculations show that this high angular momentum problem can be solved if *Theia* struck the proto-Earth obliquely at a speed comparable to the Earth's escape velocity of 11.2 km/s. So, overall the giant impact origin of the Moon succeeds in explaining a variety of geochemical and geophysical observations.

### 6.6.2 The Post-Impact Atmosphere and Loss of Volatiles

What was the effect of the Moon-forming impact on Earth's early atmosphere? If we assign a time of zero to the impact itself, essentially four environmental stages

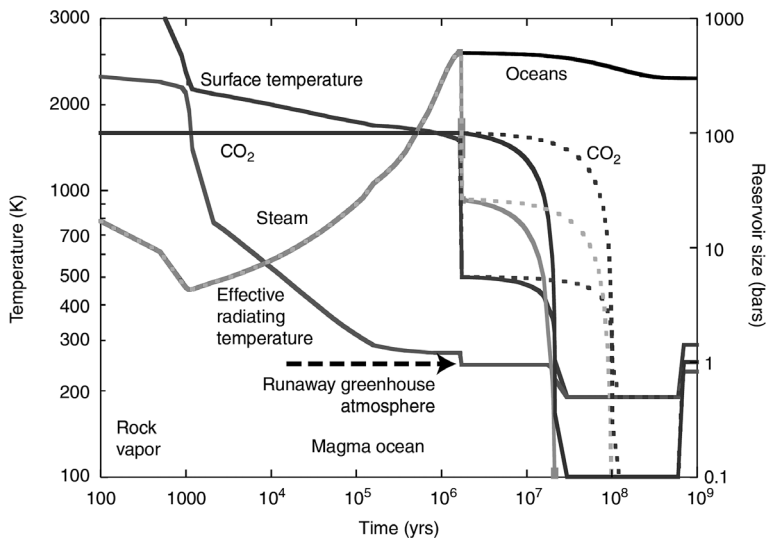


**Figure 6.17** A self-consistent model of the environmental consequences of the Moon-forming impact. See text for a description of the various phases. (From Zahnle *et al.* (2010) Reproduced with permission from Cold Spring Harbor Laboratory Press. Copyright 2010.)

should have followed (Zahnle *et al.*, 2007). These are illustrated in Fig. 6.17.

(1) From 0 to  $10^3$  years, when the atmosphere consists of a cloud of  $\sim 2500$  K vaporized rock. The most abundant atmospheric gases are SiO and  $O_2$ , but geochemical volatiles such as Na and Cl are also present in the atmosphere.

(2) From  $10^3$  to  $\sim 2$  m.y., when a deep magma ocean exists and volatiles such as water and  $CO_2$  are partitioned between the  $\sim 2000$  K melt and the atmosphere, depending on solubility. Whether the atmosphere is strongly reducing (mostly  $H_2$  and CO) or weakly reducing (mostly  $H_2O$  and  $CO_2$  with minor reducing gases) depends on how quickly the molten iron acquired from Theia sinks into the Earth's core. Generally, post impact atmospheres in equilibrium with crust or bulk silicate Earth consist mostly of  $H_2O$  and  $CO_2$  (Lupu *et al.*, 2014). Radiative cooling is controlled by steam in the atmosphere, and the atmosphere remains largely opaque to thermal infrared emanating from the surface, which maintains the high surface temperature. But eventually, the mantle starts to solidify upwards from some depth.

(3) From 2 m.y. to  $\sim 10^8$  yr: A solid surface has formed, an ocean condenses (which is salty from the Na and Cl that were once in the post-impact atmosphere), and the atmosphere consists of 100–200 bar of  $CO_2$ . The thick  $CO_2$  atmosphere is gradually removed during this period by reacting with the crust.

(4) From  $\sim 10^8$  to  $\sim 10^9$  yr: During this time, the thickness of the Hadean atmosphere is unknown. Whether the Hadean climate was green or cold depends principally on the amount of greenhouse gases because the young Sun was  $\sim 30\%$  fainter than the modern Sun. Some have

argued for a generally cold and frozen Hadean Earth because more vigorous tectonics at that time would have removed  $CO_2$  via the incorporation of  $CO_2$  into the basaltic seafloor and subsequent subduction (Sleep and Zahnle, 2001). Others suggest that much more  $CO_2$  would have been present, up to 10 bar (Walker, 1985), and that the surface could have been quite hot,  $80\text{--}90^\circ\text{C}$  (Kasting and Ackerman, 1986). The nature of Hadean climate and atmosphere remains unresolved.

Earlier, we mentioned the model of Genda and Abe (2005) for the loss of volatiles during giant impacts. Assuming that an ocean existed on the Earth before Theia hit it, their calculations suggest that the Moon-forming impact would have removed little water (Abe, 2011). However, the ocean would have been vaporized explosively, accelerating a significant fraction of the overlying atmosphere to greater than the escape velocity. Hence, most of the pre-existing atmosphere would have been blown away while the ocean would have survived. The atmosphere that emerged afterwards was thus mostly from degassed volatiles of the magma ocean formed during the impact event. Consequently, the Moon-forming impact and earlier impacts during accretion are likely to have removed any primary atmosphere by promoting its escape to space.

## 6.7 “Late Heavy Bombardment”: Causes and Consequences

After the Moon-forming impact, large bodies left over from planetary accretion were still present within the Solar System and would have caused significant impacts during the Hadean. Evidence for large impacts comes from the cratering record on the Moon and Mars. Earth

would have received  $\sim 20$  times the impactor flux of the Moon, given Earth’s larger gravity and area, so the big lunar craters imply that about a hundred  $\sim 100$ -km-diameter bodies and thousands of 10-km bodies pelted the early Earth. The timing of these impact events is debated (reviewed by Hartmann *et al.*, 2000), but arguments have been made that impacts were concentrated during the interval 4.1–3.8 Ga, which is called the *Late (Heavy) Bombardment (LHB)* or *lunar cataclysm* (Tera *et al.*, 1974). The alternative point of view, illustrated in Fig. 6.18, is that there was a smooth, exponential decline in the cratering rate back to the origin of the Moon, and that the LHB was just the tail of this decline or a statistical spike in the tail. However, very early high impact fluxes should have created huge impact basins on the surfaces of the Moon and Mars that are unseen, along with a contamination of the lunar crust with siderophile elements (such as iridium) contained in asteroids, which is also not observed. Overall, the terrestrial planets seem to have unusually large basins that formed relatively late: Imbrium and Orientale on the Moon; Hellas, Isidis, and Argyre on Mars; Rembrandt and Caloris on Mercury.

Nonetheless, evidence for the duration and magnitude of the LHB is debated (see review by Fassett and Minton (2013)). The motivation for a narrow, 100–200 m.y. LHB was a clustering of basin ages near 3.9 Ga derived from radiometric dating of lunar samples: Nectaris (3.92), Crisium (3.91), Serenitatis (3.89), and Imbrium (3.85) (Ryder *et al.*, 2000). However, *Apollo* sample radiometric

clocks appear to have been contaminated by material from the very large ( $\sim 1160$  km) Imbrium impact (Haskin, 1998; Mercer *et al.*, 2015). Moreover, data from lunar zircons and breccias suggest older impact events at 4.3–4.1 Ga (Norman *et al.*, 2010; Norman and Nemchin, 2014). On the other hand, lunar meteorites have few ages  $>4.0$  Ga (Cohen *et al.*, 2000). Also, meteorites thought to be from the  $\sim 530$  km asteroid Vesta have a spread of shock ages ranging 3.4–4.1 Ga but few from 4.4–4.1 Ga (Bogard, 1995; Marchi *et al.*, 2013). It has also been argued that the LHB is supported by a  $\sim 7$  times enhanced abundance of iridium ( $\sim 150$  ppt) in 3.8 Ga Isua sedimentary rocks compared to modern crust ( $\sim 20$  ppt) (Jorgensen *et al.*, 2009). However, contamination of Isua sedimentary rocks with basaltic debris containing  $\sim 200$  ppt Ir makes this result doubtful. Overall, the data suggest a more protracted LHB rather than a narrow interval near 3.9 Ga. In addition, impact spherules and models suggest a gradual decline of impacts in the Archean (Johnson and Melosh, 2012; Lowe *et al.*, 2014). For example, there were probably  $\sim 70$  impactors from 3.7–1.7 Ga comparable to the Chicxulub impactor (Bottke *et al.*, 2012).

Various hypotheses have been put forth to account for the LHB, all of which involve some source of planetesimals that became unstable about 600 m.y. after the Solar System formed. The most popular hypothesis has been the *Nice model*, which originated in Nice, France, and which relies on planetary migration (Gomes *et al.*, 2005). If giant planets encounter planetesimals and eject

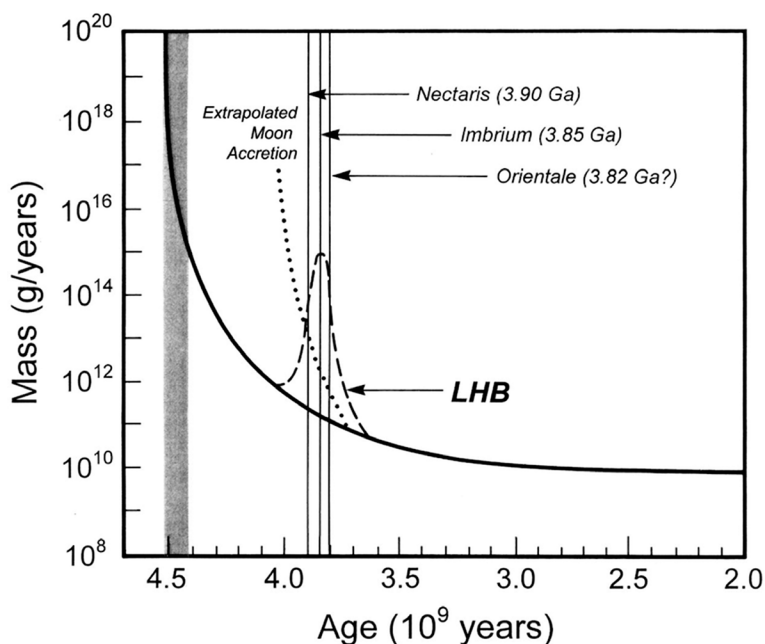


**Figure 6.18** A schematic diagram showing basic data that motivates the idea of a Late Heavy Bombardment (LHB) pulse of impacts. Ages of large lunar impact basins have been interpreted to cluster near 3.9 Ga, as shown. Backwards extrapolation of an accretion curve that includes such large impactors (dotted line) would imply accretion of Moon-sized objects ( $\sim 10^{26}$  g) at 4.1 Ga, which is unlikely; hence, the idea of a late pulse of bombardment. The solid line shows a backwards extrapolation of the current impactor flux to the origin of the Solar System. The vertical gray bar indicates the time of the formation of the Moon. (From Koeberl (2006). Reproduced with permission. Copyright 2006, Geological Society of America.)

them either in or out of the Solar System, conservation of angular momentum requires that the giant planets move slightly. The Nice model shows that for reasonable initial conditions, an evolution of orbits can cause Saturn and Jupiter to go through a 2:1 *mean motion resonance*, in which Saturn orbits the Sun once for every two Jupiter orbits. This resonance, which can occur in the models around 4.0–3.9 Ga, given appropriate initial conditions, creates a regular gravitational nudge that makes the orbits of Saturn and Jupiter more eccentric. In turn, the orbits of the other two outer planets are affected. Neptune and Uranus move outwards and themselves acquire eccentric orbits. Neptune can initially be inside the orbit of Uranus

asteroids (Chambers, 2007), and another in which Uranus and Neptune form between Jupiter and Saturn and then get scattered outwards, disturbing icy planetesimals (Thommes *et al.*, 2002).

In any case, the largest impactors of the LHB would have had a severe effect on the Earth's atmosphere, oceans and any life at the time. Essentially, the environmental consequences were similar to the Moon-forming impact, except without a magma ocean, shorter in duration, and much smaller in scale (Fig. 6.19).

Impactors larger than a certain mass,  $m_{\text{impactor}}$ , would have vaporized all the water of mass  $m_{\text{ocean}}$  in the ocean into steam, according to the following energy balance:

$$\text{kinetic energy} = (\text{heat to vaporize ocean}) + (\text{heat to reach critical temperature, } 647 \text{ K}) \quad (6.3)$$

$$\frac{1}{2}m_{\text{impactor}}v^2 = m_{\text{ocean}}L + m_{\text{ocean}}c_p\Delta T$$

and then overtake it in the migration outwards, and both planets, particularly the farthest one, scatter small icy bodies, some of which enter the inner Solar System. Meanwhile, changes in Jupiter's orbit cause resonances that increase the orbital eccentricities of asteroids, flinging some of them into the inner Solar System and expelling others entirely. Such havoc could explain several features of the Solar System: the low mass of the population of objects beyond Neptune, the low mass in the asteroid belt (~1/25 of the Moon's mass), and the LHB.

Other studies suggest that the Nice model would produce terrestrial planet eccentricities and inclinations that are larger than those observed, so that the model cannot account for the LHB (Kaib and Chambers, 2015). Other hypotheses for the LHB have been proposed, including one in which a small planet (called "Planet V") in the asteroid belt is ejected by Jupiter and produces a rain of

where  $L = 2.5 \times 10^6 \text{ J kg}^{-1}$  (at 273 K) is the latent heat of vaporization of water, and  $c_p = 1900 \text{ J kg}^{-1} \text{ K}^{-1}$  is the specific heat of water vapor. Taking the temperature change  $\Delta T = 647 \text{ K} - 273 \text{ K} = 374 \text{ K}$ , a typical asteroid collision speed of  $v = 14 \text{ km s}^{-1}$ ,  $m_{\text{ocean}} = 1.4 \times 10^{21} \text{ kg}$ , and assuming that ~1/4 of the impact energy is spent evaporating water while the rest enters the solid Earth or radiates to space, we get  $2 \times 10^{20} \text{ kg}$  for the required impactor mass. For  $3000 \text{ kg m}^{-3}$  density, the impactor is a ~500 km diameter object, similar to the asteroid Vesta (Sleep and Zahnle, 1998; Sleep *et al.*, 1989; Zahnle and Sleep, 1997). Statistically, 0–4 impactors larger than 1000 km capable of global sterilization should have hit the Earth between the Moon-forming impact and ~3.8 Ga, while 3–7 ocean-vaporizing impactors larger than 500 km should have hit (Marchi *et al.*, 2014). Each ocean vaporizing impact could potentially have sterilized the

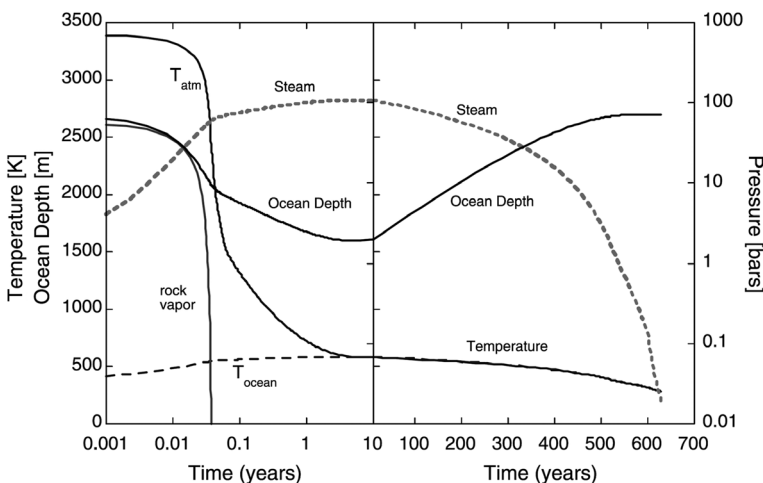


**Figure 6.19** The environmental consequences on the early Earth of an impactor that released  $10^{27} \text{ J}$ , comparable to that that caused the 2100 km-wide Hellas basin on Mars. Ocean depth, ocean temperature, and atmospheric temperature are shown as a function of time, along with the pressure of rock vapor and steam. (From Nisbet *et al.* (2007a). Reproduced with permission of Springer. Copyright 2007, Springer Science + Business Media, Inc.)

Earth, although microbes in the deep continental subsurface (if it existed) might have been able to survive (Sleep and Zahnle, 1998).

Large but non-sterilizing impacts would boil off the top tens or hundreds of meters of the ocean (Segura *et al.*, 2013). Layers of marine silica-rich sinter at  $\sim 3.3$  and 3.2 Ga could be evidence of partial ocean evaporation from such impacts (Lowe and Byerly, 2015).

The environmental consequences shown in Fig. 6.19 are for an impact comparable to that which caused the Hellas basin on Mars (2100 km wide, 8 km deep) or the lunar South-Pole Aitken crater (2500 km diameter, 13 km deep). The post-impact stages include a month with a rock vapor atmosphere that heats and evaporates seawater, making a steam atmosphere that then lasts for  $\sim 10^2$  years before radiative cooling to space causes condensation. The significances of such an event would be to devastate photosynthetic life. However, hydrothermally hosted life in the deep ocean could perhaps survive. Consequently, such impacts may explain why a comparison of genomes of organisms on Earth today suggests that the common ancestor of all life was a hyperthermophilic (“heat-loving”) microbe (Gogarten-Boekels *et al.*, 1995; Sleep *et al.*, 1989). Such microbes would have survived the LHB. Alternatively, warm hydrothermal vents might just have been good places for life to originate (Martin *et al.*, 2008).

## 6.8 The Early Atmosphere: the Effect of Planetary Differentiation and Rotation Rate

### 6.8.1 Core Formation and its Effect on Atmospheric Chemistry

The timing of differentiation of the Earth into a core, mantle, and crust had consequences for the composition of the early atmosphere. If the source region for volcanic gases was highly reducing then the gases released would have been reducing also, i.e., rich in hydrogen or hydrogen-bearing gases such as methane or ammonia. Consequently, when the proto-Earth still had metallic iron in its mantle, gases released into the atmosphere would have been very reducing, as illustrated in Fig. 6.15(a) and Fig. 6.20(a). In simple outline, once the molten iron sank to the core, the gases would have been only weakly reducing, i.e., predominantly  $\text{H}_2\text{O}$  instead of  $\text{H}_2$ , mainly  $\text{CO}_2$  instead of  $\text{CO}$  or  $\text{CH}_4$ , and  $\text{N}_2$  rather than  $\text{NH}_3$ , as shown in Fig. 6.15(b) and Fig. 6.20(b). (The actual story of the evolution of mantle oxidation state is more complex, as discussed in Ch. 7.)

Theory and geochemical data suggest that the core of the proto-Earth formed during accretion. Then, after the

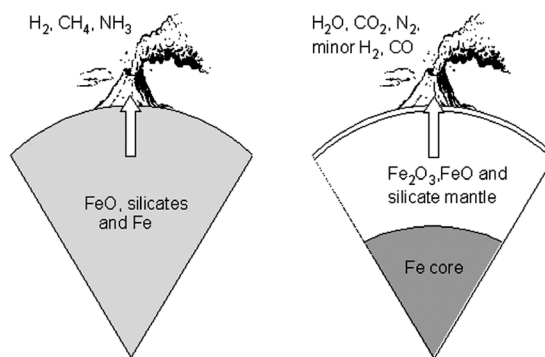


**Figure 6.20** Effect of core formation on volatiles. *Left:* Before molten iron sank from the mantle into the core, the chemical effect was to produce gases that were highly reducing. *Right:* Once the iron separated into the core, the gases would have become only weakly reducing.

Moon-forming impact, further accreted iron settled to the core quickly, so that a highly reducing atmosphere may have persisted only tens of millions of years after this impact (but see Sec. 7.3). We note that further impacts of metal-containing asteroids (i.e., the composition of ordinary or enstatite meteorites) could have generated temporary reducing atmospheres later in the Hadean, of course.

Isotopes provide clues about the rate of the Earth’s accretion and differentiation into a core and mantle (Kleine and Rudge, 2011). The most useful isotopes are radiogenic parent–daughter pairs where one element is a *siderophile*, meaning it has a tendency to separate out with molten iron, and the other is not, making it a *lithophile*. In this case, during core formation, the extent to which a radioactive lithophile remains in the mantle and the daughter product goes into the core depends on their relative affinities for iron. The now-extinct radionuclide  $^{182}\text{Hf}$  (hafnium) decays to  $^{182}\text{W}$  (tungsten) with a 9 m.y. half-life. The tungsten isotope ratio of  $^{182}\text{W}$  relative to nonradiogenic  $^{180}\text{W}$  in Earth’s mantle and crust is slightly higher than the carbonaceous chondrite value that represents primordial Solar System material. Consequently, a fraction of the Earth’s core must have formed during the 9 m.y. lifetime of the hafnium parent, because radioactive hafnium is such a strong lithophile that it remained in the mantle, which allowed the mantle, but not the core, to accumulate excess  $^{182}\text{W}$ . Core formation also decreased the mantle’s lead/uranium ratio,  $\text{Pb}/\text{U}$ , because  $\text{Pb}$  is a siderophile whereas  $\text{U}$  is not, so  $\text{Pb}$  was lost to the core. Measurements of the ratio of  $^{206}\text{Pb}$  (produced by the decay of  $^{238}\text{U}$  with a half-life of 4468 m.y.) and  $^{207}\text{Pb}$  (produced by the decay of  $^{235}\text{U}$  with a half-life of 703 m.y.) relative to nonradiogenic  $^{204}\text{Pb}$

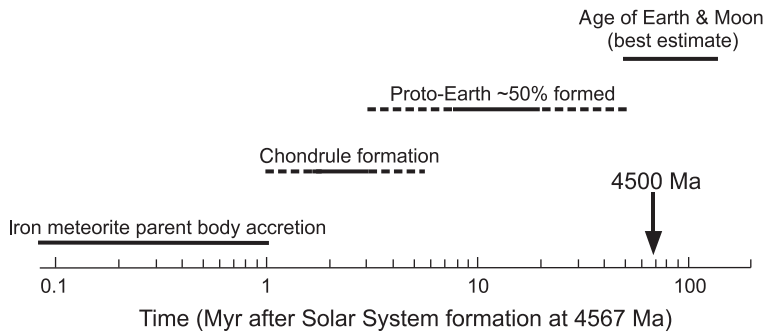


**Figure 6.21** Timescales after the formation of the Solar System, which occurred when calcium–aluminum inclusions (CAIs) formed in chondrite meteorites at 4.567 Ga. (Data from Kleine *et al.* (2011).)

suggest a segregation of lead and uranium ~50–150 m.y. after Solar System formation (Wood and Halliday, 2010).

Understanding the implications of both Hf–W and U–Pb isotope systems in detail is model-dependent. Results are determined by assumptions about whether accretion declined exponentially with time or by some other functional form, and whether the core formed in equilibrium or disequilibrium between metal and silicate. Despite these uncertainties, the data suggest that the Earth grew to 95% of its current size between 30 m.y. and 120 m.y. after Solar System formation, and that the core formed within the same period. These data are consistent with the ages of the oldest rocks on the Moon,  $4.46 \pm 0.04$  Ga (Norman *et al.*, 2003). A summary of timescales for the events in the early Solar System is shown in Fig. 6.21.

### 6.8.2 Day Length, the Lunar Orbit, and the Early Steam Atmosphere

The angular momentum of the Earth–Moon system has affected atmospheric evolution, while at the same time it is possible that the early atmosphere influenced the evolution of the angular momentum system, as we describe below. Because of tides raised in the ocean by the Moon and the friction that this exerts, the Earth's rotation rate is slowing down (Goldreich, 1966). Geology provides direct evidence. Rhythmites are stacked laminae of sandstone, siltstone and mudstone, which display periodic variations in thickness because of tidal, lunar and annual cycles (Coughenour *et al.*, 2009). Their study indicates that there were about  $400 \pm 7$  sidereal days (rotation periods) per year at ~620 Ma, consistent with a  $21.9 \pm 0.4$  hour day (Williams, 1997). Extrapolation (although not straightforward for reasons described below) would suggest that, at ~3.5 Ga, the Earth had a ~15–16 hour day. As described in Sec. 4.2, a more rapidly rotating planet would have affected the Earth's climate system through its influence on atmospheric dynamics.

The overall angular momentum of the Earth–Moon system is conserved (if we ignore angular momentum exchange with the orbit of Earth around the Sun), so as the Earth's rotation rate has declined, the angular momentum has increased in the Moon's orbit through a greater Earth–Moon distance. Essentially, the Moon has receded from the Earth as the Earth's rotational angular momentum has gradually been transferred to the Moon's orbital angular momentum.

The current lunar recession rate is  $3.82 \pm 0.07$  cm per year, which has been measured using the round-trip Earth–Moon time for laser light shined on reflectors placed on the Moon's surface by Apollo astronauts (Dickey *et al.*, 1994). This rate of recession reflects a high tidal dissipation rate on the modern Earth. The dissipation rate must have been ~3 times lower on average during the past because otherwise, running the system backwards, the Moon would have spiraled into the Earth at ~1.4 Ga (Walker *et al.*, 1983). Tidal dissipation occurs mostly when ocean waves encounter continents or shallow shelves, and hence depends critically on global geography. Unusual phenomena such as the very high tidal amplitude in the Bay of Fundy in the northwest Atlantic Ocean can contribute significantly to the dissipation rate. Fortunately, evidence from geology supports the idea that the tidal dissipation rate was slower in the past. In addition to rhythmites, there are a variety of other data. It is possible to count daily growth bands between prominent bands, interpreted as annual, in corals, bivalves and brachiopods, in order to determine the day length in the Phanerozoic (reviewed by Williams, 2000). Cyclic deposition in the Weeli Wolli Formation, Australia, which is a *banded iron formation* sedimentary rock (see Sec. 10.3.2), has also been used to estimate a day length of  $17.1 \pm 1.1$  hours at 2.45 Ga.

The effect of the early atmosphere may help solve a second conundrum of the lunar orbital evolution (Zahnle *et al.*, 2007). The Moon's orbit is currently inclined by ~5° with respect to Earth's equatorial plane (the ecliptic).

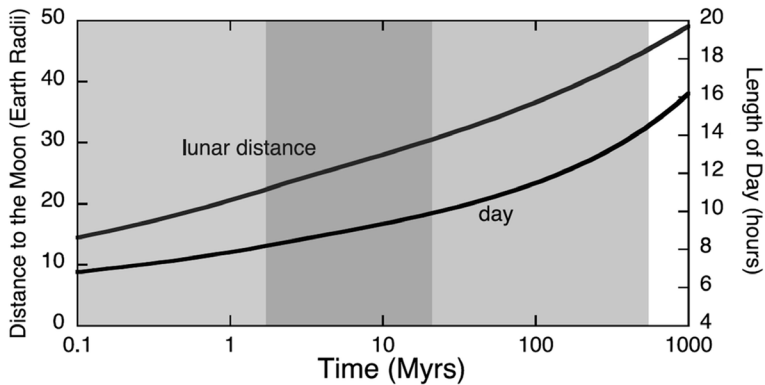


**Figure 6.22** The Earth–Moon distance (left vertical axis) and length of the Earth’s day (right vertical axis) versus time after the Moon-forming impact. The first shaded period 0.1–2 Myr corresponds to the presence of a steam atmosphere after the impact. The second shaded period corresponds to a thick CO<sub>2</sub> atmosphere that wanes with time. The third shaded period corresponds to the rest of the Hadean. The current distance to the Moon is ~60 Earth radii. (Adapted from Zahnle *et al.* (2007). Reproduced with permission of Springer. Copyright 2007, Springer Science + Business Media, B.V.)

The giant impact hypothesis predicts that the Moon should have formed within the equatorial plane, so some process must have increased its inclination. According to Touma and Wisdom (1998), this can be accomplished if the Earth–Moon system passed through two resonances that occurred soon after Moon formation. For these resonances to change the Moon’s inclination significantly, though, the Moon must have been receding much more slowly than standard theory would predict.

The problem of slower lunar recession after the Moon-forming impact can be resolved by considering the atmospheric effect of the impact on Earth’s surface and interior (Zahnle *et al.*, 2007). The impact would likely have created a molten Earth with a hot core. Tidal energy cannot be dissipated efficiently in a molten planet, which would greatly limit the rate of outward migration of the Moon. Also, the thermal blanketing of a steam atmosphere formed after the Moon-forming impact would help maintain the magma ocean by restricting the outgoing thermal radiation to space. As the mantle begins to solidify at depth, the tidal energy dissipation acting in this subsurface region would slow the freezing. But this tidal

energy could not be lost from the Earth as a whole any faster than the *runaway greenhouse* threshold set by a steam atmosphere opaque to the infrared, which is  $\sim 300 \text{ W m}^{-2}$  derived from the properties of water vapor (see Sec. 13.3.2 for an analytical derivation of this *runaway greenhouse* flux limit). The tidal heating and steam atmosphere would be coupled: the magma ocean would be maintained, while the leakage of tidal heat from the mantle would help sustain the thermal blanketing effect of the atmosphere. Eventually, slow migration of the Moon away from the Earth allowed the mantle to freeze. At this point, about 2 m.y. after the Moon forming impact, the steam greenhouse collapsed. Because of the limit on the outgoing infrared radiation set by the steam atmosphere, the evolution of the lunar orbit is slowed by a factor of 100–1000 times compared to models that ignore the effect of atmospheres and assume that tides are raised on a solid body (Zahnle *et al.*, 2007). Although 2 m.y. seems short, it is important on a logarithmic scale because this is the time when the Moon’s recession should be expected to be fastest. A possible history of the Earth’s day length and lunar distance is shown in Fig. 6.22.